Z. Angew. Math. Phys. (2016) 67:24

DOI 10.1007/s00033-015-0592-0

Zeitschrift für angewandte Mathematik und Physik ZAMP

On the whole spectrum of Timoshenko beams. Part I: a theoretical revisitation

Antonio Cazzani, Flavio Stochino and Emilio Turco

Abstract. The problem of free vibrations of the Timoshenko beam model is here addressed. A careful analysis of the governing equations allows identifying that the vibration spectrum consists of two parts, separated by a *transition frequency*, which, depending on the applied boundary conditions, might be itself part of the spectrum. For both parts of the spectrum, the values of natural frequencies are computed and the expressions of eigenmodes are provided. This allows to acknowledge that the nature of vibration modes changes when moving across the transition frequency. Among all possible combination of end constraints which can be applied to single-span beams, the case of a simply supported beam is considered. These theoretical results can be used as benchmarks for assessing the correctness of the numerical values provided by several numerical techniques, e.g. traditional Lagrangian-based finite element models or the newly developed isogeometric approach.

Mathematics Subject Classification. Primary 74K10 · 74H45 · 74H05; Secondary 70J10 · 70J30 · 34L10 · 34L15 · 35C05 · 35L25.

Keywords. Structural dynamics · Vibration analysis · Timoshenko beam · Frequency spectrum.

List of symbols

$\mathbf{A}$	Coefficient matrix for the homogenous system
$\mathbf{X}$	Unknown column matrix for the homogenous system
$\mathbf{0}$	Right-hand side column matrix for homogeneous system
A	Cross-sectional area
A_1, A_2, A_3, A_4	Integration constants for V, first part of the spectrum
B	Cross-sectional depth (and width)
B_1, B_2, B_3, B_4	Integration constants for Φ, first part of the spectrum
C_1, C_2, C_3, C_4	Integration constants for V, transition frequency
D	Constant factor [see Eq. (B.3)]
$D^\star$	Differential operator $\mathrm{d}/\mathrm{d}x$
D_1, D_2, D_3, D_4	Integration constants for Φ, transition frequency
E	Young's modulus
E_1, E_2, E_3, E_4	Integration constants for V, second part of the spectrum
E_{1n}, E_{2n}, E_{3n}, E_{4n}	Integration constants for the nth eigenmode
F_1, F_2, F_3, F_4	Integration constants for Φ, second part of the spectrum
G	Shear modulus
H, K	Amplitude of eigenmodes for double eigenvalue
I	Cross-sectional mass moment of inertia
L	Beam length
$\tilde{L}$	Special value of beam length

Published online: 02 April 2016

M	Bending moment
T	Shear force
$T^\star$	Differential operator $\mathrm{d}/\mathrm{d}t$
V	Vibration mode for transversal displacement
a	Shear stiffness
b	Transversal inertia
$\hat{b}$, $\hat{c}$	Coefficients of biquadratic wave-numbers equation
$b^\star$, $c^\star$	Coefficients of biquadratic frequency equation
c	Bending stiffness
d	Rotary inertia
f_λ	Space frequency associated with wave-number λ
f_{λ_n}	Space frequency associated with the nth vibration mode
k, k_1, k_2	Integer values corresponding to wave-numbers of vibration modes
t	Time variable
v	Transversal displacement
x	Space variable (beam abscissa)
$\hat{\Delta}$	Discriminant of wave-number equation
$\Delta^\star$	Discriminant of frequency equation
Φ	Vibration mode for section rotation
$\hat{\alpha}_1$	Coefficient of eigenmode for generalized wave-number
α_1, α_2	Eigenmode coefficients for first/second wave-number
$\tilde{\alpha}_2$	Eigenmode coefficient for second wave-number at transition frequency
κ	Shear correction factor
$\hat{\lambda}_1$	Generalized wave-number (first part of the spectrum)
λ_1	First wave-number (second part of the spectrum)
λ_2	Second wave-number (first and second part of the spectrum)
$\tilde{\lambda}_2$	Second wave-number at transition frequency
$\lambda_1^{\star 2}$	First root (squared) of wave-numbers equations
$\lambda_2^{\star 2}$	Second root (squared) of wave-numbers equations
ν	Poisson's ratio
ξ	Dimensionless space variable (dimensionless beam abscissa)
ρ	Beam density (mass per unit volume)
ϕ	Section rotation
ω	Angular frequency
$\tilde{\omega}$	Angular frequency at the transition value (cutoff frequency)
$\omega^\star$	Limiting value (upper/lower bound) for angular frequency
ω_n	Angular frequency (theoretical value) for nth vibration mode

1. Introduction

A beam model which is able to take into account both shear stiffness and rotary inertia (in addition to bending stiffness and transversal inertia, which are typical of the Euler–Bernoulli model) for structural dynamics applications was first proposed in 1921 by Timoshenko [1] and further developed in 1922 [2], and since then, it is associated with his name. A previous attempt to extend the Euler–Bernoulli [3] model by incorporating in it rotary inertia alone is ascribed to Rayleigh [4]. Together with the so-called *shear*

beam model, which descends from Timoshenko model by disregarding in it the rotary inertia contribution, these four beam models constitute the theoretical background for standard structural mechanics applications, when second- or higher-order effects can be neglected, and hence, there is no coupling between transversal and longitudinal vibrations. An interesting overview of these theories and a comparison of their applications in structural problems of engineering interest is presented in [5], while in [6] a comparison of Euler–Bernoulli and Timoshenko models with a 2-D elasticity solution is proposed. On the other hand, a variational formulation of the Timoshenko beam model has been proposed in [7,8], while a study of nonlinear vibrations has been reported in [9].

Despite the large number of papers which have appeared since 1921 on the dynamics of Timoshenko beam, there are still some issues which deserve some attention, in particular a complete and precise definition of the vibration spectrum. There is indeed much confusion about it, and several contributions, instead of helping in clarifying the topic, have instead added more incomplete pieces of information and misunderstandings. The most debated issue is the so-called *second spectrum* of Timoshenko beam theory, which was first described by Traill-Nash and Collar [10]. Following this paper, many contributions on this issue appeared; for an updated but inevitably incomplete list, at least the following works should be mentioned (in order of appearance) [11–25].

The idea of considering two spectra for the Timoshenko beam can be justified and acceptable in the framework of wave propagation, but, as long as structural vibrations are envisaged, can lead to serious misunderstandings. Indeed, looking carefully at the governing equations of motion, as it has been attempted in [26], it follows that there is a unique vibration spectrum, but with a transition between two different kinds of vibration modes. Disregarding one part of the spectrum, as some authors have claimed to do, with the motivation that it is physically unfeasible leads to contradictory conclusions. Indeed only mechanical experiments can be used to validate a theory, and in the case that experimental results do not match with the theoretical model, the latter has to be changed. Instead numerical codes implementing the Timoshenko beam model produce results which are inherently coherent with the same theory and cannot be used to validate or reject the theory itself.

As a matter of fact, most handbooks concerned with the definition of eigenmodes for the single-span Timoshenko beam model make reference only, regardless of the considered boundary conditions, to the first part of the spectrum: see, for instance, Pilkey [27, pp. 596-ff.] or Reddy [28, pp. 197–200]. Disregarding the second part of the spectrum can still be acceptable for relatively slender beams if only the first few vibration modes (e.g. <10) are required, but for shorter beams this can be unacceptable, since the transition to the second part of the spectrum, when the depth-to-span ratio is <5, as Table 1 shows, may occur around the seventh mode. Even in the rare cases when the second part of the spectrum is accounted for, e.g. in Karnowsky and Lebed [29, pp. 331-ff.], the provided solution is given in terms of complex-valued functions, which is an unnecessary complication; moreover, for the simply supported beam, the presence of the eigenmode corresponding to the transition frequency has been overlooked.

Hence, this paper is devoted to carefully developing, using only real-valued variables, the complete solution, in terms of natural frequencies and corresponding vibration modes, for the Timoshenko beam in the most general case. Results are then specialized to some peculiar boundary conditions: for these cases, the numerical values of natural frequencies and eigenmodes are constructed. These theoretical results will then be used, in a forthcoming paper [30], as suitable benchmarks to assess, from a quantitative point of view, the accuracy exhibited by some finite element models.

The rest of the paper is organized as follows: in Sect. 2, the governing equations of the dynamics of a straight Timoshenko beam are presented: in particular the decoupled fourth-order differential equations for the two components of the generalized displacement are deduced and solved. Discussion is then focused on the eigensolutions: it is shown that their nature changes when passing through a transition frequency, so that the spectrum, composed of those particular frequency values such that vibration is possible, consists of two parts with, eventually, the addition of the special value corresponding to the transition

TABLE 1. *Position within the spectrum (corresponding to $N = 10{,}000$ DOFs) of the transition frequency, $n(\tilde{\omega})$, of the first k_1-eigenmode, $n(k_1 = 1)$, number of k_1- and k_2-eigenmodes, for a simply supported Timoshenko beam having a square cross-section as a function of the length-to-depth ratio L/B for a fixed value of $a/d = 12.5 \times 10^9$ (rad/s)^2; geometric and material parameters are given in Sect. 3.1*

L/B	$n(\tilde{\omega})$	$n(k_1 = 1)$	$N(k_1)$	$N(k_2)$
1	2	4	3614	6385
2	3	5	3614	6385
5	7	8	3614	6385
10	13	14	3614	6385
20	26	27	3614	6385
50	64	65	3614	6385
100	127	128	3614	6385
200	254	255	3612	6387
500	634	635	3598	6401
1000	1268	1269	3549	6450

frequency. It has to be remarked that the analysis of the eigensolutions is performed in order to deal only with real-valued functions.

Then, in Sect. 3 modal analysis for the single-span Timoshenko beam model is presented for the simply supported beam. This is the simplest case, which has been extensively studied in the literature, and is characterized by a factorized form of the transcendental equation providing the wave-numbers associated with natural vibrations. This circumstance allows to obtain a *closed-form* expression for the vibration frequencies and produces very simple vibration modes for both part of the spectrum and the transition frequency, which is indeed part of the spectrum itself. For the analyzed case, the complete list of the first 50 natural frequencies is given for suitably chosen geometric and material data, as well as some representative plots of the eigenmodes in different portions of the spectrum; moreover, a comparison between the spectrum of the Euler–Bernoulli model and that of the Timoshenko one is presented for the same geometric and material data.

Finally in Sect. 4 some conclusions are drawn, and possible applications of the present research are exemplified. After this, some "Appendices" illustrate subtler details of the formulation, which have been omitted, for the sake of conciseness, from the main body of the paper.

A complete list of symbols has been provided for the reader's convenience.

2. The governing equations of dynamics for Timoshenko beams

For a uniform, straight Timoshenko beam, the linear and angular momentum balance equations are, respectively:

$$\frac{\partial T}{\partial x} - \rho A \frac{\partial^2 v}{\partial t^2} = 0, \tag{2.1}$$

$$\frac{\partial M}{\partial x} - T - \rho I \frac{\partial^2 \phi}{\partial t^2} = 0, \tag{2.2}$$

where T and M stand, respectively, for the transversal shear force and the bending moment; ρ is the density of the material constituting the beam; A and I are the area and the area moment of inertia of the beam cross section, while $v = v(x, t)$ and $\phi = \phi(x, t)$ are the generalized displacement of the beam, i.e. the transversal displacement of the centroid and the cross-sectional rotation, which depend on both the abscissa, x, and time, t. It is remarkable that the last terms in the left-hand side of these Eqs. (2.1) and (2.2) take into account, respectively, the transversal inertia force and the rotary inertia torque.

The adopted positive convention for internal forces and generalized displacement is shown in Fig. 1.

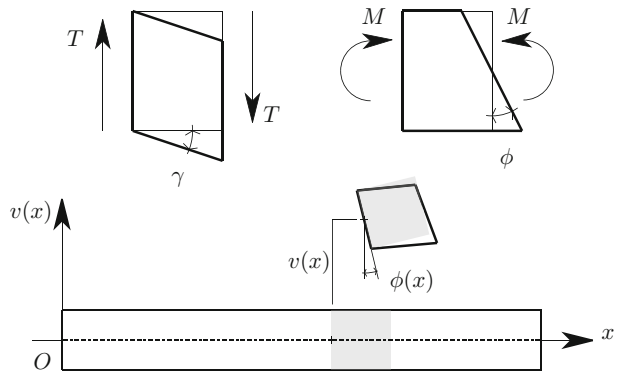

FIG. 1. Timoshenko beam element showing the assumed conventions for generalized displacements (v, ϕ) and internal forces (T, M)

The constitutive equations at the beam level, taking into account that G and E are shear and Young's moduli, and κ is the shear correction factor, read:

$$T = G\kappa A\left(\frac{\partial v}{\partial x} + \phi\right), \quad M = EI\frac{\partial \phi}{\partial x}, \tag{2.3}$$

and allow, once they are substituted into Eqs. (2.1) and (2.2), to obtain the coupled equations of motion written in terms of kinematic variables alone:

$$G\kappa A\left(\frac{\partial^2 v}{\partial x^2} + \frac{\partial \phi}{\partial x}\right) - \rho A\frac{\partial^2 v}{\partial t^2} = 0, \tag{2.4}$$

$$EI\frac{\partial^2 \phi}{\partial x^2} - G\kappa A\left(\frac{\partial v}{\partial x} + \phi\right) - \rho I\frac{\partial^2 \phi}{\partial t^2} = 0. \tag{2.5}$$

2.1. Fully decoupled equations of motion

This system of two second-order partial differential equations (PDEs) can be conveniently reduced to a unique fourth-order PDE. Toward this purpose, a symbolic form of Eqs. (2.4) and (2.5) which is suitable for operator calculus can be easily devised by defining the following shorthand notation:

$$a = G\kappa A, \quad b = \rho A, \quad c = EI, \quad d = \rho I. \tag{2.6}$$

Similarly, the following symbols are used to denote the differential operators:

$$D^\star = \frac{\partial(\cdot)}{\partial x}, \quad D^{\star 2} = \frac{\partial^2(\cdot)}{\partial x^2}, \quad \ldots, \quad D^{\star 4} = \frac{\partial^4(\cdot)}{\partial x^4}, \tag{2.7}$$

$$T^\star = \frac{\partial(\cdot)}{\partial t}, \quad T^{\star 2} = \frac{\partial^2(\cdot)}{\partial t^2}, \quad \ldots, \quad T^{\star 4} = \frac{\partial^2(\cdot)}{\partial t^4}. \tag{2.8}$$

In Eq. (2.6), a and c represent, respectively, shear and bending stiffness, while b and d are transversal and rotary inertia: the simultaneous presence of all these terms characterizes Timoshenko's beam theory. When some of them are disregarded, other beam theories (e.g. those named from Rayleigh or from Euler–Bernoulli or the so-called *shear-beam* theory) are obtained. See, for details [5,27,29].

By using the symbolic notation defined above, it results:

$$\left(aD^{\star 2} - bT^{\star 2}\right) v + aD^{\star}\phi = 0, \tag{2.9}$$

$$-aD^{\star}v + \left(cD^{\star 2} - a - dT^{\star 2}\right) \phi = 0. \tag{2.10}$$

By formal operator calculus procedures, it follows from Eq. (2.9):

$$aD^{\star}\phi = -\left(aD^{\star 2} - bT^{\star 2}\right) v, \tag{2.11}$$

which allows eliminating ϕ from Eq. (2.10), and yields the following decoupled fourth-order equation in v:

$$acD^{\star 4}v - (ad + bc)D^{\star 2}T^{\star 2}v + abT^{\star 2}v + bdT^{\star 4}v = 0. \tag{2.12}$$

After some algebraic manipulations, Eq. (2.12) can be written as follows:

$$EI\frac{\partial^4 v}{\partial x^4} - \rho I\left(1 + \frac{E}{G\kappa}\right)\frac{\partial^4 v}{\partial t^2 \partial x^2} + \rho A\frac{\partial^2 v}{\partial t^2} + \frac{\rho^2 I}{G\kappa}\frac{\partial^4 v}{\partial t^4} = 0, \tag{2.13}$$

which is the equation first established by Timoshenko [1] when developing a new beam theory able to deal with both shear strain and rotary inertia.

Similarly, if Eq. (2.11) is used this time to eliminate v and the result is substituted again into Eq. (2.10), the following decoupled fourth-order equation in ϕ is obtained:

$$acD^{\star 4}\phi - (ad + bc)D^{\star 2}T^{\star 2}\phi + abT^{\star 2}\phi + bdT^{\star 4}\phi = 0, \tag{2.14}$$

which is formally analogous to Eq. (2.12). Hence, with suitable algebraic simplifications, it comes out the fully decoupled equation of motion in terms of ϕ:

$$EI\frac{\partial^4 \phi}{\partial x^4} - \rho I\left(1 + \frac{E}{G\kappa}\right)\frac{\partial^4 \phi}{\partial t^2 \partial x^2} + \rho A\frac{\partial^2 \phi}{\partial t^2} + \frac{\rho^2 I}{G\kappa}\frac{\partial^4 \phi}{\partial t^4} = 0. \tag{2.15}$$

Remark 1. It has to be emphasized that, since Eqs. (2.13) and (2.15) are equal, as it has been already outlined by Stephen [22]—who used the same notation adopted here—also their solutions have the same form. For this reason, in the sequel attention will be focused only on solving Eq. (2.13).

2.2. Solutions of the equations of motion

Solutions to Eqs. (2.13)—or (2.15)—are sought such that independent variables, viz. x and t, are separated. In particular, it is assumed that time dependence is of a harmonic kind, so that free vibrations are possible. Thus,

$$v(x,t) = V(x)\exp(i\omega t), \quad \phi(x,t) = \Phi(x)\exp(i\omega t), \tag{2.16}$$

where $i = \sqrt{-1}$ is the imaginary unit; it follows, consequently, if primes are used to denote derivatives with respect to x:

$$\frac{\partial^4 v}{\partial x^4} = V''''(x)\exp(i\omega t), \quad \frac{\partial^4 v}{\partial t^2 \partial x^2} = -\omega^2 V''(x)\exp(i\omega t),$$

$$\frac{\partial^2 v}{\partial t^2} = -\omega^2 V(x)\exp(i\omega t), \quad \frac{\partial^4 v}{\partial t^4} = +\omega^4 V(x)\exp(i\omega t), \tag{2.17}$$

with analogous expressions for the derivatives of $\phi(x,t)$. If Eq. (2.17) are substituted into Eq. (2.13), the common time factors are simplified and the coefficient of the highest derivative in the resulting ordinary differential equation (ODE) is selected to have a unit value, and it results:

$$V'''' + \frac{\rho\omega^2}{E}\left(1+\frac{E}{G\kappa}\right)V'' + \frac{\rho\omega^2}{E}\left(\frac{\rho\omega^2}{G\kappa}-\frac{A}{I}\right)V = 0. \tag{2.18}$$

This is a fourth-order ODE with constant coefficients, whose solutions are to be found in the form of exponential functions $V(x)=\exp(\lambda^\star x)$, where, in general, $\lambda^\star \in \mathbb{C}$.

Then $V''=\lambda^{\star 2}\exp(\lambda^\star x)$ and $V''''=\lambda^{\star 4}\exp(\lambda^\star x)$; after substituting these values and performing some cancelations, this characteristic equation is arrived at:

$$\lambda^{\star 4} + \hat{b}\lambda^{\star 2} + \hat{c} = 0, \tag{2.19}$$

i.e. a biquadratic algebraic equation, whose independent variable is $\lambda^\star$; for conciseness reasons, the following notation has been adopted:

$$\hat{b} = \frac{\rho\omega^2}{E}\left(1+\frac{E}{G\kappa}\right) = \omega^2\frac{d}{c}\left(1+\frac{bc}{ad}\right), \tag{2.20}$$

$$\hat{c} = \frac{\rho\omega^2}{E}\left(\frac{\rho\omega^2}{G\kappa}-\frac{A}{I}\right) = \omega^2\frac{d}{c}\left(\omega^2\frac{b}{a}-\frac{b}{d}\right). \tag{2.21}$$

The squared roots of Eq. (2.19) are therefore:

$$\lambda_1^{\star 2} = \frac{1}{2}\left(-\hat{b}+\sqrt{\hat{b}^2-4\hat{c}}\right), \quad \lambda_2^{\star 2} = \frac{1}{2}\left(-\hat{b}-\sqrt{\hat{b}^2-4\hat{c}}\right). \tag{2.22}$$

2.3. Analysis of the eigensolutions

Based on the value of the transition frequency,

$$\tilde{\omega}^2 = \frac{G\kappa A}{\rho I} = \frac{a}{d}, \tag{2.23}$$

when solving Eq. (2.19), these three cases must be distinguished, as it is shown in detail in Appendix A.

Case 1: $\omega^2 < \tilde{\omega}^2$. From the analysis presented in Appendix A, for this angular frequency range it results: $\lambda_1^{\star 2} > 0$ and $\lambda_2^{\star 2} < 0$.

As a consequence, Eq. (2.19) has *two real roots*, namely $\pm\sqrt{\lambda_1^{\star 2}}$, and *two purely imaginary conjugate roots* viz. $\pm i\sqrt{-\lambda_2^{\star 2}}$.

Case 2: $\omega^2 = \tilde{\omega}^2$. In the present case, by the same analysis developed in Appendix A, it follows: $\lambda_1^{\star 2} = 0$ and $\lambda_2^{\star 2} < 0$. In particular,

$$\lambda_2^{\star 2} = -\hat{b}|_{\omega^2=\tilde{\omega}^2} = -\left(\frac{G\kappa A}{EI}+\frac{A}{I}\right) = -\left(\frac{a}{c}+\frac{b}{d}\right). \tag{2.24}$$

Consequently, there is *a null real root, whose multiplicity is two*, and *one couple of imaginary conjugate roots*, namely again $\pm i\sqrt{-\lambda_2^{\star 2}}$.

Case 3: $\omega^2 > \tilde{\omega}^2$. This time it results $\lambda_1^{\star 2} < 0$ and $\lambda_2^{\star 2} < 0$.

As a consequence, *all four roots* of Eq. (2.19) *are purely imaginary*. In particular, there are *two couples of conjugate roots*, i.e. $\pm i\sqrt{-\lambda_1^{\star 2}}$ and $\pm i\sqrt{-\lambda_2^{\star 2}}$.

Remark 2. The value $\tilde{\omega}^2$ given by Eq. (2.23) represents, from the physical point of view, the ratio between shear stiffness and rotary inertia.

Physical reasons show that $G\kappa A > 0$, $\rho I > 0$, so that $\tilde{\omega} = \sqrt{\tilde{\omega}^2} \in \mathbb{R}^+$ and such value can be attained indeed: it is the value of the *cutoff frequency* of waves propagating in an infinite Timoshenko beam, as it is shown, for instance, in Graff [31, pp. 185–187].

In the analysis presented here, such frequency represents a *transition value* between two different solutions of the ODE, Eq. (2.18); moreover, this transition value might itself be or might be not part of the frequency spectrum, depending on the applied boundary conditions.

2.4. The eigenmodes of Timoshenko beams

The analysis developed in Sect. 2.3 allows identifying, in terms of real-valued quantities only, the complete solution to Eq. (2.18) and the corresponding equation which provides $\Phi(x)$.

Results will be presented separately for the three cases outlined above.

Case 1: $\omega^2 < \tilde{\omega}^2$. The eigenfunctions in terms of $V(x)$ and $\Phi(x)$ are:

$$V(x) = A_1 \cosh \hat{\lambda}_1 x + A_2 \sinh \hat{\lambda}_1 x + A_3 \cos \lambda_2 x + A_4 \sin \lambda_2 x, \tag{2.25}$$

$$\Phi(x) = B_1 \cosh \hat{\lambda}_1 x + B_2 \sinh \hat{\lambda}_1 x + B_3 \cos \lambda_2 x + B_4 \sin \lambda_2 x, \tag{2.26}$$

where the following *proper* (λ_2) and *generalized* ($\hat{\lambda}_1$) wave-numbers apply:

$$\hat{\lambda}_1 = +\sqrt{\lambda_1^{\star 2}}, \quad \lambda_2 = +\sqrt{-\lambda_2^{\star 2}}. \tag{2.27}$$

Indeed, λ_2, which appears in the argument of a trigonometric function, is a *true* wave-number: it gives the measure of the portion, measured in radians, of sine/cosine waves which appear in a unit length of the beam. By analogy, $\hat{\lambda}_1$, which is part of the argument of an hyperbolic function (which reduces to a trigonometric function for imaginary values of its argument), will be defined a *generalized* wave-number. On the other hand, the number of *complete* sine/cosine waves which appear in a unit length of the beam define the *space frequency*, $f_\lambda = \lambda/(2\pi)$, as a complete wave has a length equal to 2π.

Looking at Eq. (2.26), it is clear that coefficients $B_1, \ldots, B_4$ depend on $A_1, \ldots, A_4$ because of Eq. (2.11), so that after some lengthy algebra it results:

$$\begin{aligned} \Phi(x) = &-\frac{\hat{\alpha}_1}{\hat{\lambda}_1}\left(A_2 \cosh \hat{\lambda}_1 x + A_1 \sinh \hat{\lambda}_1 x\right) \\ &+ \frac{\alpha_2}{\lambda_2}\left(A_4 \cos \lambda_2 x - A_3 \sin \lambda_2 x\right). \end{aligned} \tag{2.28}$$

In Eq. (2.28), the following shorthand notation has been adopted:

$$\hat{\alpha}_1 = \omega^2 \frac{b}{a} + \hat{\lambda}_1^2, \quad \alpha_2 = \omega^2 \frac{b}{a} - \lambda_2^2. \tag{2.29}$$

Case 2: $\omega^2 = \tilde{\omega}^2$. Since in this case $\lambda_1^{\star 2} = 0$, $\lambda_2^{\star 2} = -\tilde{\lambda}_2^2$, it follows that, see Eqs. (2.6) and (2.24):

$$\tilde{\lambda}_2 = \sqrt{\left(\frac{G\kappa A}{EI} + \frac{A}{I}\right)} = \sqrt{\left(\frac{a}{c} + \frac{b}{d}\right)}. \tag{2.30}$$

Then the eigenfunctions have these expressions:

$$V(x) = C_1 + C_2\frac{x}{L} + C_3\cos\tilde{\lambda}_2 x + C_4\sin\tilde{\lambda}_2 x, \tag{2.31}$$

$$\Phi(x) = D_1 + C_2\frac{x}{L} + D_3\cos\tilde{\lambda}_2 x + D_4\sin\tilde{\lambda}_2 x, \tag{2.32}$$

where L is the beam length. In this way, all coefficients $C_1,\ldots,C_4$ (and, similarly, $D_1,\ldots,D_4$) are dimensionally homogeneous, as in the previous case, see Eqs. (2.25) and (2.26). However, in the present case, there is only one wave-number, namely $\tilde{\lambda}_2$.

Again, the coefficients appearing in Eqs. (2.31) and (2.32) are not independent, since Eqs. (2.9) and (2.10) hold. By making again use of Eq. (2.11), it is possible to identify those terms having the same functional dependence on x. In particular, it results:

$$\frac{1}{L}D_2 + \tilde{\omega}^2\frac{b}{a}C_1 = 0, \quad \tilde{\omega}^2\frac{b}{a}\frac{1}{L}C_2 = 0,$$
$$\tilde{\lambda}_2\left(D_4 - \tilde{\lambda}_2 C_3\right) + \tilde{\omega}^2\frac{b}{a}C_3 = 0, \quad \tilde{\lambda}_2\left(D_3 + \tilde{\lambda}_2 C_4\right) - \tilde{\omega}^2\frac{b}{a}C_4 = 0.$$

Therefore, these are the explicit links between the two sets of coefficients:

$$D_2 = -\tilde{\omega}^2\frac{b}{a}C_1 L, \quad C_2 = 0, \quad D_3 = \frac{\tilde{\alpha}_2}{\tilde{\lambda}_2}C_4, \quad D_4 = -\frac{\tilde{\alpha}_2}{\tilde{\lambda}_2}C_3, \tag{2.33}$$

where, for the sake of a compact notation, the following definition has been adopted—see also Eqs. (2.23), (2.30):

$$\tilde{\alpha}_2 = \tilde{\omega}^2\frac{b}{a} - \tilde{\lambda}_2^2 = -\frac{a}{c}. \tag{2.34}$$

Therefore, in the present case, the complete solution in terms of eigenmodes is:

$$V(x) = C_1 + C_3\cos\tilde{\lambda}_2 x + C_4\sin\tilde{\lambda}_2 x, \tag{2.35}$$

$$\Phi(x) = D_1 - \tilde{\omega}^2\frac{b}{a}C_1 x - \frac{\tilde{\alpha}_2}{\tilde{\lambda}_2}\left(C_3\sin\tilde{\lambda}_2 x - C_4\cos\tilde{\lambda}_2 x\right). \tag{2.36}$$

Remark 3. The complete solution of the ODEs which define $V(x)$ and $\Phi(x)$ must depend only on *four* independent coefficients, since these equations descend from a system of two second-order PDEs, Eqs. (2.4) and (2.5). This, however, does not require that *both* V and Φ *have to depend on four coefficients each*, as it is clearly shown in Eqs. (2.35) and (2.36). In particular, the circumstance that $C_2 = 0$ follows directly from the kinematic condition expressed by Eq. (2.11).

On the other hand, if Eq. (2.10) is used instead of Eq. (2.9), it can be easily checked that while the same conditions given by Eq. (2.33) are recovered for C_2, D_3, D_4, the value of D_2 remains undefined, since $V(x)$ appears in Eq. (2.10) only with its first derivative with respect to x, and consequently, coefficient C_1 does not appear explicitly.

Case 3: $\omega^2 > \tilde{\omega}^2$. In this last case, the eigenfunctions are:

$$V(x) = E_1\cos\lambda_1 x + E_2\sin\lambda_1 x + E_3\cos\lambda_2 x + E_4\sin\lambda_2 x, \tag{2.37}$$

$$\Phi(x) = F_1\cos\lambda_1 x + F_2\sin\lambda_1 x + F_3\cos\lambda_2 x + F_4\sin\lambda_2 x, \tag{2.38}$$

where the two independent, real-valued wave-numbers are given by:

$$\lambda_1 = +\sqrt{-\lambda_1^{\star 2}}, \quad \lambda_2 = +\sqrt{-\lambda_2^{\star 2}}. \tag{2.39}$$

Table 2. *Basic end constraints for a single-span Timoshenko beam*

Constraint	Symbol	Constrained variables	Equivalent kinematic constraints
Clamped (or fixed)	C	$V = 0$ and $\Phi = 0$	$V = 0$ and $\Phi = 0$
Free	F	$T = 0$ and $M = 0$	$V' + \Phi = 0$ and $\Phi' = 0$
Guided	G	$T = 0$ and $\Phi = 0$	$V' = 0$ and $\Phi = 0$
Supported (or hinged)	S	$V = 0$ and $M = 0$	$V = 0$ and $\Phi' = 0$

A prime indicates a derivative with respect to x: $\Phi' = \mathrm{d}\Phi/\mathrm{d}x$; $V' = \mathrm{d}V/\mathrm{d}x$

Again, coefficients $F_1, \ldots, F_4$ depend on $E_1, \ldots, E_4$ because of Eq. (2.11), so that after some algebraic manipulations one gets:

$$\Phi(x) = \frac{\alpha_1}{\lambda_1}\left(E_2 \cos \lambda_1 x - E_1 \sin \lambda_1 x\right) + \frac{\alpha_2}{\lambda_2}\left(E_4 \cos \lambda_2 x - E_3 \sin \lambda_2 x\right), \tag{2.40}$$

where the following shorthand notation has been adopted:

$$\alpha_1 = \omega^2 \frac{b}{a} - \lambda_1^2, \tag{2.41}$$

while α_2 is still defined by Eq. $(2.29)_2$.

3. Modal analysis of Timoshenko beams

In this Section, modal analysis of a Timoshenko beam is developed, in order to devise its complete spectrum.

The results of Sect. 2 clearly show that the complete spectrum, *regardless of the boundary conditions*, must be constructed by taking into account that it consists of two portions, *none of which can be disregarded*.

In the first part of the spectrum, which is relevant to natural frequencies $\omega_n < \tilde{\omega}$, the eigenmodes are given, in general, by a linear combination of hyperbolic and trigonometric functions, see Eqs. (2.25) and (2.28). Only for particular choices of boundary conditions (BCs), it is possible to annihilate the contribution of hyperbolic functions: this happens, for instance, in the case of a simply supported beam.

In the second part of the spectrum, corresponding to natural frequencies $\omega_n > \tilde{\omega}$, modal shapes are instead given by a linear combination of trigonometric functions having two different wave-numbers, λ_1 and λ_2, as Eqs. (2.37) and (2.40) show. Again, in general, these eigenmodes involve both λ_1 and λ_2, since wave-numbers are entwined (or even entangled); only for particular cases, e.g. the simply supported beam, the contributions of wave-numbers become decoupled.

Moreover, even the transition frequency, $\tilde{\omega}$, might belong to the spectrum, and hence, this condition has to be taken into account, too. If the transition frequency is part of the spectrum, modal shapes are given by a linear combination of trigonometric functions depending *on just one wave-number*, $\tilde{\lambda}_2$ and of a constant function (for V), see Eq. (2.35), or a linear combination of trigonometric functions and a complete linear polynomial (for Φ), as Eq. (2.36) shows.

In any case, the particular blending of the above-mentioned functions which provides the actual eigenmode depends on the applied BCs.

For a single-span beam, as long as transversal vibrations only are envisaged, four basic end constraints might be encountered: clamped (or fixed), free, guided and supported (or hinged). The corresponding constrained variables in the homogeneous case (perfect constraints) as well as the equivalent kinematic constraints are listed in Table 2.

With these four basic constraints, it is possible to devise ten different combinations of single-span constrained beams, provided that combinations where the constraints are simply reversed (e.g. C–F and F–G) are counted only once. These are: clamped–clamped (or *doubly clamped*, C–C), clamped–free (C–F),

clamped–guided (C–G), clamped–supported (C–S); free–free (F–F), free–guided (F–G), free–supported (F–S); guided–guided (G–G), guided–supported (G–S); supported–supported (or *simply supported*, S–S).

For the sake of simplicity, the spectrum will be explicitly computed here only for the simply supported beam, while in a companion paper [32] the doubly clamped (C–C) beam will be considered: that is somehow representative of all other cases which can occur.

However, only in the case of a simply supported beam, the wave-number transcendental equation can be written in a factorized form, and as a consequence, the frequency equation becomes a simple algebraic equation, e.g. Eq. (3.13), and allows for the evaluation of natural frequencies ω_n by a direct method. Moreover, the simply supported beam is the only case where the transition frequency is *always* part of the spectrum.

Instead, in all the remaining cases, since the wave-number transcendental equation cannot be written as a product, there is a complete coupling: indeed, in the first part of the spectrum, hyperbolic functions appear in the eigenmodes, while, in the second part of the spectrum, each eigenmode is represented by a combination of trigonometric functions which depend on *both* wave-numbers. Then, the computation of natural frequencies ω_n must be performed by solving a complicated implicit transcendental equation.

The transcendental equation corresponding to several other BCs can be found, for instance, in [14], where only those which are valid for $\omega_n < \tilde{\omega}$ are reported, and in [5], where the complete expressions are given, although they are written in an unnecessarily involved way.

3.1. Material and geometric data

Since it is not possible to provide the spectrum of a *generic* Timoshenko beam, attention has been focused on a particular beam, which from the physical point of view has reasonable (i.e. not pathological) geometric and mechanical data. On the other hand, once theoretical details are clear, it is a simple exercise changing the data to build the spectrum for other simply supported beams made of different materials or having different length and/or cross-sectional shapes.

The case which has been analyzed is the following: a straight uniform and homogeneous beam, whose length is $L = 2\,\mathrm{m}$, having a square cross section with side length (either depth or width) $B = 0.1\,\mathrm{m}$; as a consequence, the cross-sectional area and area moment of inertia are, respectively, $A = B^2 = 0.01\,\mathrm{m}^2$; $I = B^4/12 = 1/120{,}000\,\mathrm{m}^4$. Moreover, the length-to-depth ratio (a rough measure of slenderness) is in this case: $L/B = 20$.

Material density is assumed to be $\rho = 8000\,\mathrm{kg/m}^3$, Young's modulus $E = 260\,\mathrm{GPa}$, (i.e. $E = 260 \times 10^3\,\mathrm{N/mm}^2$), Poisson's ratio $\nu = 0.3$ so that, under the hypothesis of elastic isotropy, the shear modulus is $G = 100\,\mathrm{GPa}$.

The last parameter, namely the shear correction factor, has been chosen according to the standard value (first adopted by Goens [33], and based on results obtained in 1897 by Föppl [34] with an elementary strain energy method), given for static analysis of a rectangular cross section:

$$\kappa = 5/6. \tag{3.1}$$

In the literature (see, for further Refs. [35–39]) for dynamic analyses, a value depending also on Poisson's ratio has been suggested: in particular for a rectangular cross section, one should choose either:

$$\kappa = \frac{10(1+\nu)}{(12+11\nu)}, \tag{3.2}$$

which was proposed by Cowper [40], or

$$\kappa = \frac{5(1+\nu)}{(6+5\nu)}. \tag{3.3}$$

This was originally proposed by Higuchi et al. [41] and later endorsed by Hutchinson [42]; according to [43–45] it provides a better agreement with 2-D elasticity solutions in the dynamic range.

It is patent that for a vanishing value of the Poisson's ratio, all the above equations provide the same value, coinciding with Eq. (3.1). Moreover, as a matter of fact, when computing the value of the transition frequency for the considered beam by adopting $\kappa = 5/6$, the value given by Eq. (3.1), the result is $\tilde{\omega} = 111{,}803.39887\,\mathrm{rad/s}$; for $\kappa = 130/153$, i.e. the value provided by Eq. (3.2), the result becomes $\tilde{\omega} = 112{,}894.18957\,\mathrm{rad/s}$ (almost 1 % more than the previous one); finally by the last Eq. (3.2), it is $\kappa = 13/15$ and the result changes to $\tilde{\omega} = 114{,}017.54251\,\mathrm{rad/s}$, i.e. <2 % of the first one: the influence of the choice of κ is really small.

For this reason, and since the interest is that of comparing for *one and the same* problem, the theoretical frequency values with those come out from suitable numerical methods, e.g. the traditional displacement-based finite element method (FEM) and the new spline-based isogeometric analysis (IGA), without the need of matching experimental results (as it has been done by Rosinger and Ritchie [46]), there are no particular reasons for preferring for κ the values given by Eqs. (3.2) and (3.3), instead of the simpler one, Eq. (3.1).

3.2. The case of a simply supported beam

For such a beam, whose length is L, the boundary conditions require that (see Table 2):

$$@x = 0: \quad V = 0 \quad \text{and} \quad M = 0; \quad @x = L: \quad V = 0 \quad \text{and} \quad M = 0. \tag{3.4}$$

By virtue of Eq. $(2.3)_2$ the homogeneous condition $M(x) = 0$ is equivalent to imposing $\Phi'(x) = 0$. It follows then:

1. for $\omega^2 < \tilde{\omega}^2$:

$$\Phi'(x) = -\hat{\alpha}_1 \left(A_1 \cosh \hat{\lambda}_1 x + A_2 \sinh \hat{\lambda}_1 x \right) - \alpha_2 \left(A_3 \cos \lambda_2 x + A_4 \sin \lambda_2 x \right). \tag{3.5}$$

2. for $\omega^2 = \tilde{\omega}^2$:

$$\Phi'(x) = -\tilde{\omega}^2 \frac{b}{a} C_1 - \tilde{\alpha}_2 \left(C_3 \cos \tilde{\lambda}_2 x + C_4 \sin \tilde{\lambda}_2 x \right). \tag{3.6}$$

3. for $\omega^2 > \tilde{\omega}^2$:

$$\Phi'(x) = -\alpha_1 \left(E_1 \cos \lambda_1 x + E_2 \sin \lambda_1 x \right) - \alpha_2 \left(E_3 \cos \lambda_2 x + E_4 \sin \lambda_2 x \right). \tag{3.7}$$

In what follows, the two parts of the spectrum and the transition frequency will be treated separately.

3.2.1. First part of the spectrum: $\omega^2 < \tilde{\omega}^2$. When BCs are substituted into Eqs. (2.25) and (3.5), the following homogeneous system of simultaneous linear algebraic equations is obtained:

$$\mathbf{A}\mathbf{X} = \mathbf{0}, \tag{3.8}$$

where the square matrix $\mathbf{A}$ and the column vectors $\mathbf{X}$ and $\mathbf{0}$ have these expressions:

$$\mathbf{A} = \begin{bmatrix} 1 & 0 & 1 & 0 \\ \hat{\alpha}_1 & 0 & \alpha_2 & 0 \\ \cosh \hat{\lambda}_1 L & \sinh \hat{\lambda}_1 L & \cos \lambda_2 L & \sin \lambda_2 L \\ \hat{\alpha}_1 \cosh \hat{\lambda}_1 L & \hat{\alpha}_1 \sinh \hat{\lambda}_1 L & \alpha_2 \cos \lambda_2 L & \alpha_2 \sin \lambda_2 L \end{bmatrix}, \quad \mathbf{X} = \begin{Bmatrix} A_1 \\ A_2 \\ A_3 \\ A_4 \end{Bmatrix}, \quad \mathbf{0} = \begin{Bmatrix} 0 \\ 0 \\ 0 \\ 0 \end{Bmatrix}. \tag{3.9}$$

Since, as a simple check confirms, $\hat{\alpha}_1 - \alpha_2 = \hat{\lambda}_1^2 + \lambda_2^2 > 0$, it follows $A_1 = 0$; $A_3 = 0$ and this reduced system of equations is obtained:

$$\begin{bmatrix} \sinh \hat{\lambda}_1 L & \sin \lambda_2 L \\ \hat{\alpha}_1 \sinh \hat{\lambda}_1 L & \alpha_2 \sin \lambda_2 L \end{bmatrix} \begin{Bmatrix} A_2 \\ A_4 \end{Bmatrix} = \begin{Bmatrix} 0 \\ 0 \end{Bmatrix}. \tag{3.10}$$

Non-trivial solutions to this reduced matrix problem exist provided that $(\alpha_2 - \hat{\alpha}_1)\sinh\hat{\lambda}_1 L \sin\lambda_2 L = 0$, i.e. being $\hat{\alpha}_1 - \alpha_2 \neq 0$, when the following transcendental equation is satisfied:

$$\sinh\hat{\lambda}_1 L \sin\lambda_2 L = 0. \tag{3.11}$$

By the rule which ensures the vanishing of a product, it must be:

$$\hat{\lambda}_1 L = 0 \quad \text{or} \quad \lambda_2 L = k_2\pi, \quad (k_2 \in \mathbb{N}). \tag{3.12}$$

The former occurrence has to be disregarded since it implies, for $L \neq 0$ (the alternative $L = 0$ being unfeasible for physical reasons), by Eq. $(2.27)_1$ that $\lambda_1^{\star 2} = 0$ and this only occurs when the natural frequency is precisely equal to the transition frequency $\omega = \tilde{\omega}$, but then solution is ruled by Case 2, which is treated below, in Sect. 3.2.2.

The latter occurrence gives, for $L \neq 0$, $\lambda_2 = k_2\pi/L$, and yields (details are given in Appendix B) the following *frequency equation* for the simply supported Timoshenko beam:

$$\omega^4 + b^\star\omega^2 + c^\star = 0. \tag{3.13}$$

This Eq. (3.13), which was obtained for the first time in [1], can also be found in [14]: there, however, it has been deduced without a complete discussion like that presented here, and led the authors to some misleading comments about the second part of the spectrum.

Equation (3.13) is again a biquadratic one, whose squared solutions are:

$$\omega_1^2 = \frac{1}{2}\left(-b^\star + \sqrt{b^{\star 2} - 4c^\star}\right), \quad \omega_2^2 = \frac{1}{2}\left(-b^\star - \sqrt{b^{\star 2} - 4c^\star}\right). \tag{3.14}$$

The analysis of the solutions to Eq. (3.13) proceeds with the same procedure presented in Sect. 2.3; the details are given in Appendix C.

Synthetically, these conclusions can be drawn:

1. since the discriminant $\Delta^\star = b^{\star 2} - 4c^\star > 0$, it results that the squared solutions of biquadratic equation (3.13), see Eq. (3.14), are such that $\omega_1^2 \in \mathbb{R}$, $\omega_2^2 \in \mathbb{R}$; moreover, both of them turn out to be positive;
2. hence Eq. (3.13) admits four real roots, namely $\pm\sqrt{\omega_1^2}$, $\pm\sqrt{\omega_2^2}$; since negative values of frequency are physically meaningless, possible vibration modes are identified by either $\omega_n = \sqrt{\omega_1^2}$ or $\omega_n = \sqrt{\omega_2^2}$;
3. however, in the first part of the spectrum, the frequency of vibration must also comply with these restrictions:

$$\omega_n < \tilde{\omega} \quad \text{and} \quad \omega_n < \omega_{k_2}^\star, \tag{3.15}$$

which descends immediately from (B.4), so that the only *admissible solutions* are of the kind:

$$\omega_n = \omega_{k_2} = +\sqrt{\omega_2^2(k_2)}, \quad (k_2 = 1, \ldots, k_2^\star), \tag{3.16}$$

with

$$k_2^\star = \max\{k_2 \in \mathbb{N} | \omega_{k_2} < \tilde{\omega}\}. \tag{3.17}$$

The meaning of Eq. (3.16) is that the k_2th frequency is given by the positive root of Eq. $(3.14)_2$ once the value $k_2\pi/L$ has been plugged into (3.13).

Thus, by virtue of (3.16) the natural frequency for the first part of the spectrum is completely identified; the definition of the corresponding eigenmodes, $V_n(x) = V_{k_2}(x)$, $\Phi_n(x) = \Phi_{k_2}(x)$, follows immediately from Eqs. (3.8)–(3.10), taking into account that $A_{1n} = 0$; $A_{3n} = 0$ and considering that when $\lambda_2 L = k_2\pi$ it follows from Eq. (3.12) $\sinh\hat{\lambda}_1 L \neq 0$, which implies $A_{2n} = 0$.

Then, by assuming that the eigenfunctions are normalized so that $V_n(x) = V_{k_2}(x)$ has a unit value when it reaches its absolute maximum, which means $A_{4n} = 1$, one finds:

$$V_{k_2}(x) = \sin\lambda_2 x; \quad \Phi_{k_2}(x) = \frac{\alpha_2}{\lambda_2}\cos\lambda_2 x, \tag{3.18}$$

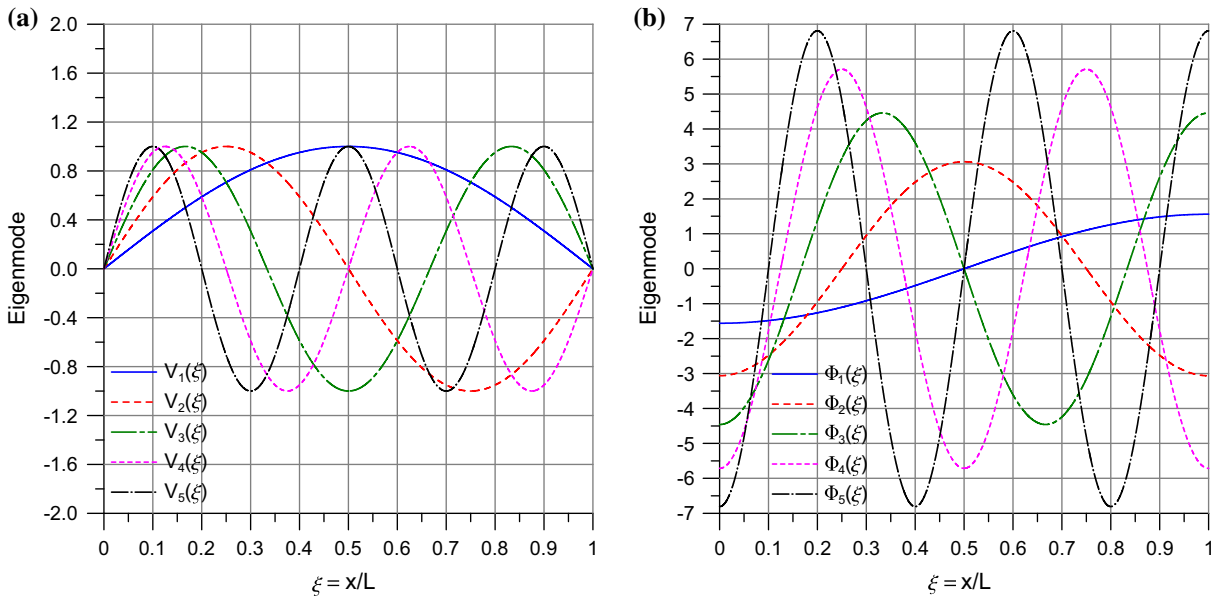

FIG. 2. Vibration shapes corresponding to modes 1–5 for a simply supported Timoshenko beam, *first* part of the spectrum. **a** Transversal displacement, V. **b** Section rotation, Φ. Geometric and material data are given in Sect. 3.1

where integer index k_2 belongs to this range:

$$k_2 = 1, \ldots, k_2^\star. \tag{3.19}$$

It has to be emphasized that in Eq. (3.18) $\lambda_2 = \lambda_2(\omega_{k_2})$ and $\alpha_2 = \alpha_2(\omega_{k_2})$ i.e. they assume the values corresponding to ω_{k_2}. The plots of the first eigenmodes which are relevant to the first part of the spectrum are shown in Fig. 2.

3.2.2. Transition frequency: $\omega^2 = \tilde{\omega}^2$. When BCs are substituted into Eqs. (2.35) and (3.6), a new homogeneous system of simultaneous linear algebraic equations similar to Eq. (3.8) is obtained; however, since in this case $\lambda_1^{\star 2} = 0$, the square matrix $\mathbf{A}$ and the column matrix $\mathbf{X}$ are now given by:

$$\mathbf{A} = \begin{bmatrix} 1 & 1 & 0 & 0 \\ \tilde{\omega}^2 \frac{b}{a} & \tilde{\alpha}_2 & 0 & 0 \\ 1 & \cos \tilde{\lambda}_2 L & \sin \tilde{\lambda}_2 L & 0 \\ \tilde{\omega}^2 \frac{b}{a} & \tilde{\alpha}_2 \cos \tilde{\lambda}_2 L & \tilde{\alpha}_2 \sin \tilde{\lambda}_2 L & 0 \end{bmatrix}, \quad \mathbf{X} = \begin{Bmatrix} C_1 \\ C_3 \\ C_4 \\ D_1 \end{Bmatrix}, \tag{3.20}$$

where, by Eq. (2.30), $\tilde{\lambda}_2 = \sqrt{-\lambda_2^{\star 2}|_{\omega=\tilde{\omega}}}$, and by Eq. (2.34):

$$\tilde{\alpha}_2 = \tilde{\omega}^2 \frac{b}{a} - \tilde{\lambda}_2^2 = -\frac{a}{c}.$$

The coefficient matrix $\mathbf{A}$ appearing in Eq. (3.20) has never $\operatorname{rank}(\mathbf{A}) > 3$. This implies that the homogeneous system of equations is defective, and this is clearly seen, since it does not depend on coefficient D_1.

Therefore if the above-mentioned matrix has precisely $\operatorname{rank}(\mathbf{A}) = 3$, i.e., taking advantage of Eq. (2.34) to simplify the resulting expression:

$$\left(\tilde{\alpha}_2 - \tilde{\omega}^2 \frac{b}{a}\right) \sin \tilde{\lambda}_2 L = -\tilde{\lambda}_2^2 \sin \tilde{\lambda}_2 L \neq 0, \tag{3.21}$$

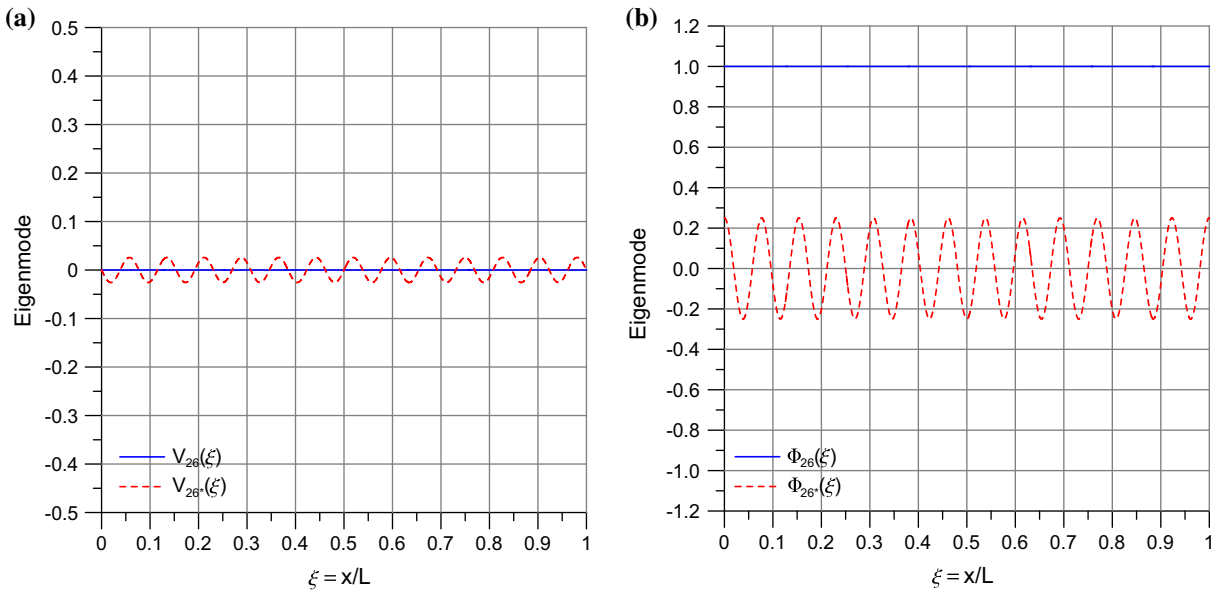

FIG. 3. Vibration shapes corresponding to the *transition frequency* (mode 26) for a simply supported Timoshenko beam. Transversal displacement, V, is shown in **a**; section rotation, Φ in **b**. The vibration modes for the case of a double eigenmode (which corresponds to a length $\tilde{L} = 2.0519240731$ m) are marked by *dashed lines*. Geometric and material data are given in Sect. 3.1

then the only non-trivial solutions to problem (3.8) (when Eq. (3.20) holds) are given by $C_1 = C_{1\tilde{\omega}} = 0$, $C_3 = C_{3\tilde{\omega}} = 0$, $C_4 = C_{4\tilde{\omega}} = 0$ and $D_1 = D_{1\tilde{\omega}} \neq 0$; in particular the eigenfunction can be normalized so that $D_{1\tilde{\omega}} = 1$.

The eigenfunction for $\omega^2 = \tilde{\omega}^2$ and $\sin \tilde{\lambda}_2 L \neq 0$ is hence:

$$V_{\tilde{\omega}}(x) = 0, \quad \Phi_{\tilde{\omega}}(x) = 1. \tag{3.22}$$

The mode described by Eq. (3.22) consists of a *pure-shear* vibration mode (see Fig. 3, solid line plots), where transversal displacement is always zero, while section rotation assumes a constant value, which is the same for all cross sections: this ensures that flexural effects do not enter into the play. Vibrations of Timoshenko beams for this transition frequency, resulting in no transverse deflection, have been first studied by Downs [11].

Instead, when the coefficient matrix $\mathbf{A}$ of Eq. (3.20) has $\text{rank}(\mathbf{A}) < 3$, i.e. when

$$\tilde{\lambda}_2^2 \sin \tilde{\lambda}_2 L = 0, \tag{3.23}$$

this implies that the beam length L has a particular value:

$$L = \tilde{L} = \frac{\tilde{k}\pi}{\tilde{\lambda}_2}, \quad \tilde{k} \in \mathbb{N}, \tag{3.24}$$

such that $\sin \tilde{\lambda}_2 \tilde{L} = 0$. Then for $\omega = \tilde{\omega}$ there is a *double eigenvalue*. This condition corresponds to a length $\tilde{L}$ such that an integer number of sine waves can fit within the beam length, thus satisfying all BCs; then the space frequency $f_\lambda = f_{\tilde{\lambda}_2} = \tilde{\lambda}_2 \tilde{L}/(2\pi) = \tilde{k}/2$ turns out to be an integer number (when $\tilde{k}$ is even) or a half-integer one (when $\tilde{k}$ is odd). As a consequence, non-trivial solutions to problem (3.8) (when Eq. (3.20) holds) are given by $C_1 = C_{1\tilde{\omega}} = 0$, $C_3 = C_{3\tilde{\omega}} = 0$ while $C_4 = C_{4\tilde{\omega}} \neq 0$ and $D_1 = D_{1\tilde{\omega}} \neq 0$; in particular, the eigenfunction corresponding to the transition frequency depends on *two arbitrarily chosen* amplitudes $D_{1\tilde{\omega}} = H$, $C_{4\tilde{\omega}} = K$, which correspond to two different eigenmodes.

Hence, for the case rank($\mathbf{A}$) < 3 (which occurs when $\omega^2 = \tilde{\omega}^2$ and $\sin \tilde{\lambda}_2 L = 0$), the two eigenfunctions can be written synthetically as:

$$V_{\tilde{\omega}}(x) = K \sin \tilde{\lambda}_2 x, \quad \Phi_{\tilde{\omega}}(x) = H + \frac{\tilde{\alpha}_2}{\tilde{\lambda}_2} K \cos \tilde{\lambda}_2 x. \tag{3.25}$$

This is shown again in Fig. 3, where the eigenfunctions corresponding to the repeated eigenvalue are plotted (for the particular choice $K = \tilde{\lambda}_2/(5\tilde{\alpha}_2)$, to improve legibility) with a dashed line.

Remark 4. The eigenmode corresponding to Eq. (3.22) is *not* a rigid-body mode, since it corresponds to a frequency value $\omega = \tilde{\omega} \neq 0$, and this shows that to produce a constant cross-sectional rotation, it is indeed required to have shear strain.

On the other hand, the appearance of this pure-shear vibration mode can be prevented by BCs: so, if both ends of the beam are clamped and not simply supported, this eigenmode does not appear, and the transition frequency $\tilde{\omega}$ is not, in general, part of the spectrum, unless the beam has a specific length $\tilde{L}$. This point will be addressed in [32].

3.2.3. Second part of the spectrum: $\omega^2 > \tilde{\omega}^2$. In this case, substitution of the BCs into Eqs. (2.37) and (3.7) gives a homogeneous system of simultaneous linear algebraic equations which is analogous to Eq. (3.8), but with these definitions of the square matrix $\mathbf{A}$ and of the column matrix $\mathbf{X}$:

$$\mathbf{A} = \begin{bmatrix} 1 & 0 & 1 & 0 \\ \alpha_1 & 0 & \alpha_2 & 0 \\ \cos \lambda_1 L & \sin \lambda_1 L & \cos \lambda_2 L & \sin \lambda_2 L \\ \alpha_1 \cos \lambda_1 L & \alpha_1 \sin \lambda_1 L & \alpha_2 \cos \lambda_2 L & \alpha_2 \sin \lambda_2 L \end{bmatrix}, \quad \mathbf{X} = \begin{Bmatrix} E_1 \\ E_2 \\ E_3 \\ E_4 \end{Bmatrix}. \tag{3.26}$$

By taking into account Eqs. (2.22), (2.29)$_2$ and (2.41), it is an easy task checking that $\alpha_2 - \alpha_1 = {\lambda_1}^2 - \lambda_2^2 = \lambda_2^{\star 2} - \lambda_1^{\star 2} = -\sqrt{\hat{\Delta}} < 0$. It follows from here $E_1 = 0$; $E_3 = 0$ and Eq. (3.8) can be reduced to:

$$\begin{bmatrix} \sin \lambda_1 L & \sin \lambda_2 L \\ \alpha_1 \sin \lambda_1 L & \alpha_2 \sin \lambda_2 L \end{bmatrix} \begin{Bmatrix} E_2 \\ E_4 \end{Bmatrix} = \begin{Bmatrix} 0 \\ 0 \end{Bmatrix}. \tag{3.27}$$

Non-trivial solutions exist provided that $(\alpha_2 - \alpha_1) \sin \lambda_1 L \sin \lambda_2 L = 0$, i.e., being $\alpha_1 - \alpha_2 \neq 0$, when the following transcendental equation is satisfied:

$$\sin \lambda_1 L \sin \lambda_2 L = 0. \tag{3.28}$$

In order to satisfy Eq. (3.28), it must be:

$$\lambda_1 L = k_1 \pi \quad \text{or} \quad \lambda_2 L = k_2 \pi, \quad (k_1, k_2 \in \mathbb{N}). \tag{3.29}$$

The former occurrence implies in this case, for $L \neq 0$, the condition

$$\lambda_1 = k_1 \frac{\pi}{L},$$

which can be satisfied by an infinite sequence of integer indices, $k_1 \in \mathbb{N}$. Again, $k_1 = 0$ has to be discarded since it would give $\lambda_1 = 0$ and that brings back to the transition frequency case, see Sect. 3.2.2.

In order to find the admissible solutions for λ_1, it is possible to obtain again the frequency equation for the simply supported beam, see Eq. (3.13). Details are given in Appendix D.

The same discussion of Eq. (3.13) presented in Sect. 3.2.1 and the findings reported in Appendix C apply here, too, with suitable changes. In particular, these conclusions are outlined:

1. Eq. (3.13) admits in this case four real roots, namely $\pm\sqrt{\omega_1^2}$, $\pm\sqrt{\omega_2^2}$; if negative values of frequency are disregarded as physically meaningless, possible vibration modes are identified by either $\omega_n = \sqrt{\omega_1^2}$ or $\omega_n = \sqrt{\omega_2^2}$;

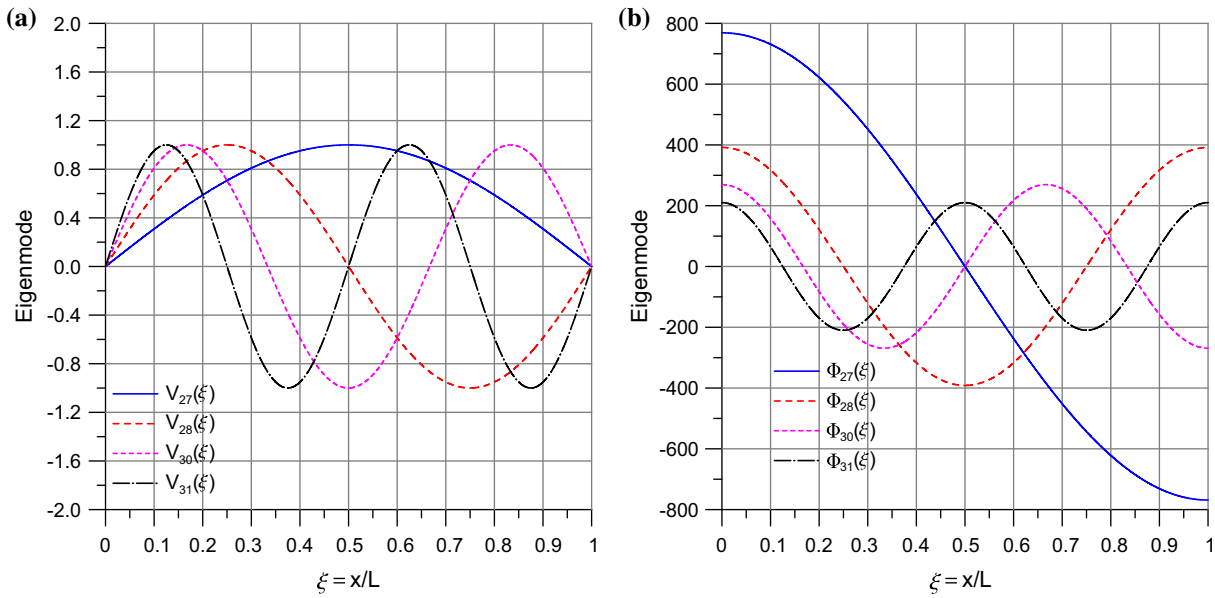

FIG. 4. Vibration shapes corresponding to λ_1 wave-numbers: modes 27, 28, 30, 31 for a simply supported Timoshenko beam, *second* part of the spectrum. Transversal displacement, V, is shown in **a**; section rotation, Φ in **b**. Geometric and material data are given in Sect. 3.1

2. however, in this second part of the spectrum, the frequency of vibration must also comply with these restrictions:

$$\omega_n > \tilde{\omega} \quad \text{and} \quad {\omega_n}^2 > {\omega_{k_1}^\star}^2, \tag{3.30}$$

so that only solutions of this kind are *admissible*:

$$\omega_n = \omega_{k_1} = +\sqrt{\omega_1^2(k_1)}, \tag{3.31}$$

where the lower bound ${\omega_{k_1}^\star}^2$ is defined by Eq. (D.3).

The notation employed in Eq. (3.31) means that the solution in terms of frequency is given by the positive root of ω_1^2, once the value $k_1\pi/L$ has been plugged into it. It has to be noticed that in Eq. (3.31) the integer index k_1 takes values inside this range:

$$k_1 = 1, \ldots, \infty. \tag{3.32}$$

By virtue of (3.31), the natural frequency for this first contribution to the second part of the spectrum is completely identified; the definition of the corresponding eigenmodes, $V_n(x) = V_{k_1}(x)$, $\Phi_n(x) = \Phi_{k_1}(x)$, follows immediately from Eq. (3.8) (when Eq. (3.26) holds), taking into account that $E_{1n} = 0$; $E_{3n} = 0$ and considering that when $\lambda_1 L = k_1\pi$ it follows from Eq. (3.27) $E_{4n} = 0$, since $\sin\lambda_2 L \neq 0$. Then, by assuming a suitable normalization for the eigenfunction, namely $E_{2n} = 1$, one finds:

$$V_{k_1}(x) = \sin\lambda_1 x, \quad \Phi_{k_1}(x) = \frac{\alpha_1}{\lambda_1}\cos\lambda_1 x, \tag{3.33}$$

where index k_1 takes the values defined by the range (3.32), while in Eq. (3.33) $\lambda_1 = \lambda_1(\omega_{k_1})$ and $\alpha_1 = \alpha_1(\omega_{k_1})$, i.e. they assume the values corresponding to ω_{k_1}.

Some illustrative examples of these eigenmodes are presented in Fig. 4; differently from what happens in Fig. 5, here low wave-numbers are encountered, as in the first part of the spectrum: for comparison purposes, and to outline significant differences, the reader should also look over Fig. 2.

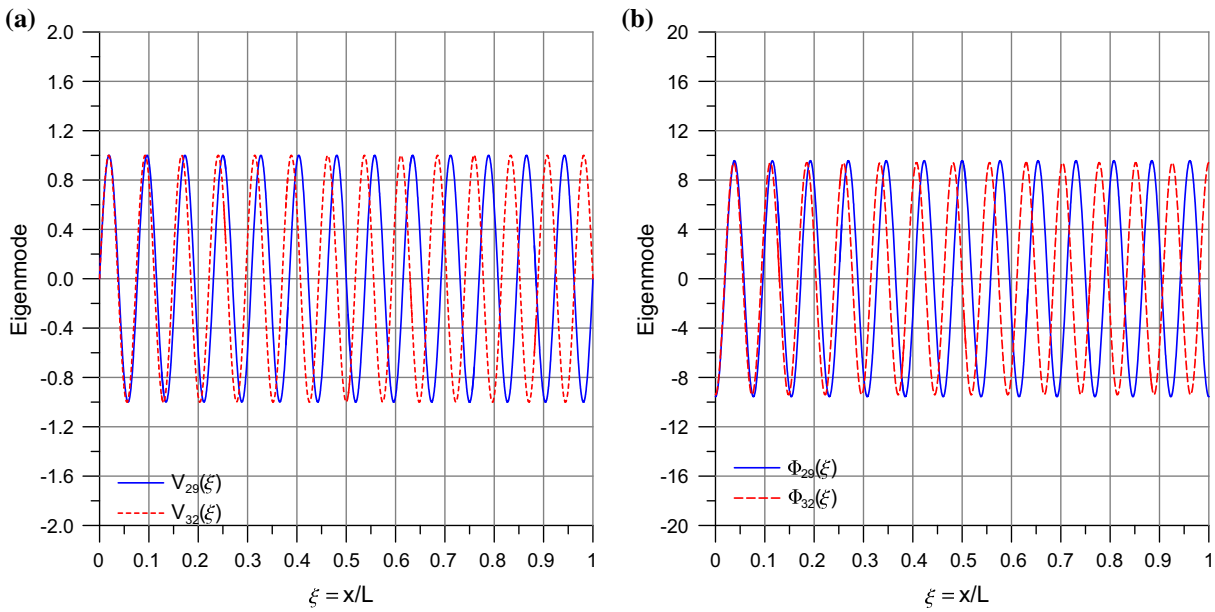

FIG. 5. Vibration shapes corresponding to λ_2 wave-numbers: modes 29 and 32 for a simply supported Timoshenko beam, *second* part of the spectrum. Transversal displacement, V, is shown in **a**; section rotation, Φ in **b**. Geometric and material data are given in Sect. 3.1

The latter occurrence [see Eq. (3.29)] gives, for $L \neq 0$:

$$\lambda_2 = k_2 \frac{\pi}{L},$$

and provides, see e.g. Eq. (B.1) the *same* solution already discussed in Sect. 3.2.1:

$$\omega_n = \omega_{k_2} = +\sqrt{\omega_2^2(k_2)}, \quad k_2 = k_2^\star + 1, \ldots, \infty, \tag{3.34}$$

with the only remarkable difference that, being now $\omega > \tilde{\omega}$, index k_2 must take values in a range which extends beyond the value $k_2^\star$ which has been defined in Eq. (3.17). On the other hand, the upper bound for $\omega_{k_2}^2$ represented by Eq. (B.4) has still to be satisfied: indeed, if it is violated, no valid solutions are found to Eq. $(3.14)_2$.

As a consequence, since for $\sin \lambda_2 L$ the solution to problem (3.8) (when Eq. (3.26) holds) is given by $E_{2n} = 0$ and $E_{4n} \neq 0$, if the same normalization is assumed, e.g. $E_{4n} = 1$, the relevant eigenmodes, provided that index k_2 is in the suitable range defined by Eq. $(3.34)_2$, are:

$$V_{k_2}(x) = \sin \lambda_2 x, \quad \Phi_{k_2}(x) = \frac{\alpha_2}{\lambda_2} \cos \lambda_2 x, \tag{3.35}$$

which still coincide with Eq. (3.18), holding in the first part of the spectrum. It can be checked that this circumstance occurs only in case of a simply supported beam: other combinations of BCs never produce eigenmodes having the same shape in the first and in the second part of the spectrum. Some illustrative examples of these eigenmodes are presented in Fig. 5: it should be remarked that they are always associated with *higher* wave-numbers than the corresponding eigenmodes, which are relevant to the first part of the spectrum (see Fig. 2).

3.3. Construction of the spectrum for the simply supported beam

Having performed the complete analysis for free vibrations of a simply supported Timoshenko beam, it has been acknowledged that the frequency spectrum consists of two parts, separated by a transition frequency,

$$\tilde{\omega} = \sqrt{G\kappa A/\left(\rho I\right)},$$

coinciding, as already pointed out in Remark 2, with the cutoff frequency for wave propagation in an infinite Timoshenko beam.

In the first part of the spectrum, frequencies are given by Eq. (3.16), and the corresponding eigenmodes by Eq. (3.18).

In correspondence with the *transition frequency*, $\omega_n = \tilde{\omega}$, which for a simply supported beam happens to be part of the spectrum, the eigenmode is described by Eq. (3.22) (or by Eq. (3.25), for those particular values of the beam length such that there is a double eigenvalue corresponding to $\tilde{\omega}$).

Finally in the second part of the spectrum, there are *two sets* of frequencies, namely:

1. the extension of the previous one, see Eq. (3.34), depending on the λ_2 wave-number, whose eigenmodes are still given by Eq. (3.18);
2. a brand new one, depending on the λ_1 wave-number, which is peculiar of this part of the spectrum, where frequencies are determined by Eq. (3.31) and eigenmodes by Eq. (3.33).

The two sets of frequencies are in this case decoupled, differently from what happens for other combinations of BCs, in the sense that either an eigenmode depends exclusively on the λ_1 wave-number, or it depends solely on the λ_2 one.

In order to proceed to the construction of the spectrum, it is necessary to provide explicitly the material and geometric data of the beam.

Differently from the dynamics of Euler–Bernoulli beam, where the natural frequencies $\omega_{k,EB}$ (and the corresponding eigenmodes $V(x)_{k,EB}$) have very simple expressions for a simply supported beam:

$$\omega_{k,EB} = (k\pi)^2\omega^\star, \quad \omega^\star = \sqrt{\frac{EI}{\rho A}}, \quad V(x)_{k,EB} = \sin\left(\frac{k\pi}{L}x\right), \tag{3.36}$$

and this property allows to build directly the spectrum for the most general case (and in a very general way) as a function of *one dimensionless parameter alone*, $\omega^\star$, here such a method cannot be adopted since there are *several independent parameters*.

It is however possible to realize that the transition frequency $\tilde{\omega}$, which allows splitting the spectrum in two parts, depends *only* on the ratio a/d between shear stiffness and rotary inertia and is *independent* of the beam length. Once these parameters are known, it is possible to evaluate it once for all: if the beam length L changes, it is possible to show that $\tilde{\omega}$ *remains fixed*, while the spectrum moves to the right (when L increases) or to the left (if L decreases). For very short beams, it comes out that the transition frequency might correspond to the first mode and the first part of the spectrum vanishes; on the other hand, the longer the beam, the more extended the first part of the spectrum becomes. The second part of the spectrum, however, never vanishes.

Some quantitative results of the transition mode as a function of the length-to-depth ratio L/B for a uniform beam having a square cross section (having a side length B) at a fixed value of the a/d ratio, see Eq. (2.6), are presented in Table 1. In particular, the position of the transition frequency $\tilde{\omega}$ and of the eigenmode corresponding to $k_1 = 1$, Eq. (3.29), within the spectrum, as well as the number of modes (denoted, respectively, by $N(k_1)$ and $N(k_2)$ corresponding to the λ_1 and the λ_2 wave-numbers is listed there.

Remark 5. A change of vibration modes is peculiar, as it has been shown, of Timoshenko beam theory; however, even for the simpler Euler–Bernoulli beam theory, a transition between different eigenmodes

TABLE 3. *Computed natural frequencies, wave-numbers and vibration amplitudes of a simply supported Timoshenko beam for the first $N = 50$ vibration modes: first part of the spectrum and transition frequency*

n	k_1	k_2	ω_n	λ_n	f_{λ_n}	A_{4n} (C_{1n})	B_{3n} (D_{1n})
1	–	1	404.3540829	1.570796327	0.25	1.	−1.560803807
2	–	2	1597.560957	3.141592654	0.50	1.	−3.063603135
3	–	3	3524.348082	4.712388980	0.75	1.	−4.459349847
4	–	4	6104.920320	6.283185307	1.00	1.	−5.713740857
5	–	5	9247.993743	7.853981634	1.25	1.	−6.808596292
6	–	6	1286.193645	9.424777961	1.50	1.	−7.739727835
7	–	7	16,862.12383	10.99557429	1.75	1.	−8.513139409
8	–	8	21,174.58318	12.56637061	2.00	1.	−9.141129809
9	–	9	25,736.94981	14.13716694	2.25	1.	−9.639130208
10	–	10	30,497.85749	15.70796327	2.50	1.	−10.02349276
11	–	11	35,415.60971	17.27875959	2.75	1.	−10.31011820
12	–	12	40,456.65009	18.84955592	3.00	1.	−10.51370482
13	–	13	45,594.10054	20.42035225	3.25	1.	−10.64741053
14	–	14	50,806.48035	21.99114858	3.50	1.	−10.72276712
15	–	15	56,076.63514	23.56194490	3.75	1.	−10.74973665
16	–	16	61,390.86478	25.13274123	4.00	1.	−10.73683943
17	–	17	66,738.22381	26.70353756	4.25	1.	−10.69131113
18	–	18	72,109.96465	28.27433388	4.50	1.	−10.61926501
19	–	19	77,499.09604	29.84513021	4.75	1.	−10.52584612
20	–	20	82,900.03304	31.41592654	5.00	1.	−10.41537176
21	–	21	88,308.31933	32.98672286	5.25	1.	−10.29145567
22	–	22	93,720.40640	34.55751919	5.50	1.	−10.15711606
23	–	23	99,133.47750	36.12831552	5.75	1.	−10.01486857
24	–	24	104,545.3068	37.69911184	6.00	1.	−9.866805432
25	–	25	109,954.1463	39.26990817	6.25	1.	−9.714662773
26	–	–	111,803.3989	–	–	0.	1.000000000

Circular frequency, ω_n is expressed in rad/s, wave-number, λ_n, in rad/m, space frequency, $f_{\lambda_n} = \lambda_n/(2\pi)$ in m^{-1}; all other parameters are dimensionless

can occur, for instance, when the beam is partly supported by an elastic foundation. This phenomenon has been thoroughly studied in [47–49]. Other, more complicated transitions (involving more than one frequency) occur when dealing with modal analysis of plates, either treated by a 2-D elasticity theory [50] or by Reissner–Mindlin theory [51].

3.3.1. Comments on the vibration frequency spectrum. With the above-mentioned data, it has been possible to compute the spectrum of natural frequencies for the simply supported Timoshenko beam up to the first $N = 10{,}000$ modes; the first $N = 50$ of them have been extracted and are reported in Tables 3 and 4. The transition frequency occurs in this case for $\tilde{\omega} = 111{,}803.3989$ rad/s, and it happens to be the 26th mode. The interested readers may request the authors for the computer code for computing the natural frequencies for any value of N and for any other geometric and material data.

Looking at the complete list of natural frequencies and at the reduced one (see Tables 3, 4), it is interesting to outline these issues:

1. For the chosen beam length, the first part of the spectrum encompasses the first 25 natural modes, all of them corresponding to the λ_2 wave-number (k_2-eigenmodes) defined by Eq. (3.18). Above the transition frequencies, where the $\tilde{\omega}$-eigenmode is given by Eq. (3.22), there appear, irregularly interspersed with the k_2-eigenmodes, the natural modes corresponding to the λ_1 wave-number: the k_1-eigenmodes, which are defined by Eq. (3.33). The first two of them, corresponding to $k_1 = 1$, $k_1 = 2$, occupy positions 27th and 28th in the above-mentioned list.
2. For the same values of the k_1 and k_2 indices, the corresponding wave-numbers are equal: this is due to the same form of Eq. (3.29); however, the corresponding natural frequencies ω_{k_1} and ω_{k_2}

TABLE 4. *Computed natural frequencies, wave-numbers and vibration amplitudes of a simply supported Timoshenko beam for the first $N = 50$ vibration modes, second part of the spectrum frequency*

n	k_1	k_2	ω_n	λ_n	f_{λ_n}	E_{2n} or E_{4n}	F_{1n} or F_{3n}
27	1	–	112,275.2383	1.570796327	0.25	1.	768.8346189
28	2	–	113,670.6573	3.141592654	0.50	1.	391.6956430
29	–	26	115,358.6353	40.84070450	6.50	1.	−9.559877425
30	3	–	115,933.6562	4.712388980	0.75	1.	269.0975234
31	4	–	118,983.2427	6.283185307	1.00	1.	210.0200254
32	–	27	120,757.7263	42.41150082	6.75	1.	−9.403634895
33	5	–	122,726.4860	7.853981634	1.25	1.	176.2477827
34	–	28	126,150.6263	43.98229715	7.00	1.	−9.246909765
35	6	–	127,069.6867	9.424777961	1.50	1.	155.0442116
36	–	29	131,536.7480	45.55309348	7.25	1.	−9.090499676
37	7	–	131,925.7658	10.99557429	1.75	1.	140.9585750
38	–	30	136,915.6711	47.12388980	7.50	1.	−8.935053917
39	8	–	137,217.9485	12.56637061	2.00	1.	131.2748014
40	–	31	142,287.1097	48.69468613	7.75	1.	−8.781097464
41	9	–	142,880.7632	14.13716694	2.25	1.	124.4925604
42	–	32	147,650.8870	50.26548246	8.00	1.	−8.629051189
43	10	–	148,859.4765	15.70796327	2.50	1.	119.7187476
44	–	33	153,006.9133	51.83627878	8.25	1.	−8.479248853
45	11	–	155,108.8098	17.27875959	2.75	1.	116.3905182
46	–	34	158,355.1690	53.40707511	8.50	1.	−8.331951400
47	12	–	161,591.4548	18.84955592	3.00	1.	114.1367406
48	–	35	163,695.6901	54.97787144	8.75	1.	−8.187358974
49	13	–	168,276.6548	20.42035225	3.25	1.	112.7034594
50	–	36	169,028.5563	56.54866776	9.00	1.	−8.045621043

Circular frequency, ω_n is expressed in rad/s, wave-number, λ_n, in rad/m, space frequency, $f_{\lambda_n} = \lambda_n/(2\pi)$ in m^{-1}; all other parameters are dimensionless

descend from different solutions of Eq. (3.13) and are therefore different. In particular, ω_{k_1} is given by Eq. (3.31), while ω_{k_2} comes out from either Eqs. (3.16) or (3.34).

3. Looking at the coefficients of the components $\Phi_{k_1}(x)$ and $\Phi_{k_2}(x)$ of the eigenmodes, it results that in all cases $\alpha_1/\lambda_1 > 0$, while $\alpha_2/\lambda_2 < 0$.
   This means that in the former case, namely the k_1-eigenmodes, the *section rotation* $\Phi(x)$ and the *slope of the transversal displacement*, $\mathrm{d}V(x)/\mathrm{d}x$, have the same sign, i.e. *their contributions to the total shear strain*, see Eq. $(2.3)_1$, *simply sum up*, while in the latter case, that corresponding to the k_2-eigenmodes, section rotation and slope of the transversal displacement have opposite sign, so that *the relevant contributions to the total shear strain partly cancel each other*.
   Such property had been already detected by Stephen [22, pp. 378–379], even though the explanation which was given there appears rather obscure and unnecessarily complicated.
4. For the chosen mechanical and geometric data, when a total number N of natural frequencies is fixed, the composition of the spectrum in terms of k_1-eigenmodes and k_2-eigenmodes presents a fairly constant ratio. For instance if $N = 100$ is chosen (i.e. the first 100 natural frequencies are considered), there are 33 k_1-eigenmodes and 66 k_2-eigenmodes (plus, of course, the mode corresponding to the *transition frequency* $\tilde{\omega}$); for $N = 500$ the same numbers become 180 and 319; similarly, for $N = 1000$ one gets 361 and 638; for $N = 5000$, 1807 and 3192; for $N = 10{,}000$, 3614 and 6385.

For comparison purpose, the full spectrum relevant to the first 100 vibration modes for both Euler–Bernoulli's and the Timoshenko's beam is shown in Fig. 6: it is apparent that in the latter case the vibration frequencies are much less separated than in the former one. This is due to the appearance, in the spectrum of Timoshenko beam, of two independent wave-numbers, which are somehow entwined.

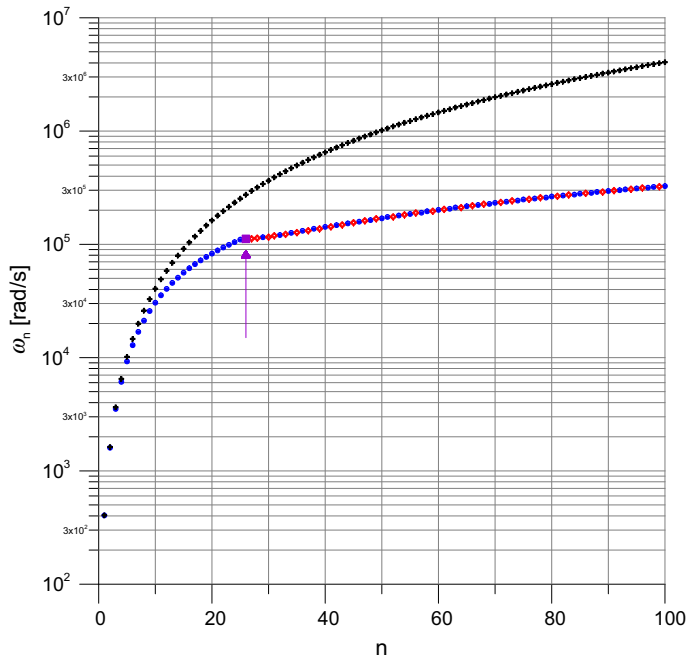

FIG. 6. Full frequency spectrum, i.e. ω_n vs. n plot (for $N = 100$ modes) for the simply supported Euler–Bernoulli beam model (denoted by *crosses*) and for the Timoshenko one. For the latter, modes corresponding to λ_2 wave-numbers are marked by *solid dots*, modes corresponding to λ_1 wave-numbers are denoted by *hollow diamonds*, while the transition frequency is shown by a *solid square*: a *vertical arrow* indicates its position

4. Conclusion

A complete analysis of the equations of motion for the Timoshenko beam model has been presented in the case of free vibrations. This has brought some important results in understanding the nature of the vibration spectrum, which has often been overlooked in the past. A careful analysis reveals indeed that there is a transition frequency such that eigenmodes corresponding to natural frequencies lying below or above it exhibit a rather different shape; moreover, the transition frequency itself might be part of the spectrum, producing a peculiar vibration mode. As a consequence, the vibration spectrum of a Timoshenko beam has to be acknowledged to be unique, but consisting of two parts, none of which can be, in principle, disregarded.

Specific attention has been devoted to the special case of a simply supported beam: the transcendental equation which provides the wave-numbers corresponding to natural frequencies is factorized, and this property produces vibration modes which have in both part of the spectrum (excluding the transition frequency, whose eigenmode is characterized by a constant function) a simple shape, consisting of an integer number of sine/cosine half-waves.

For the given mechanical and geometric data (which are representative of a beam model where shear strain effects are expected to be non-negligible), a complete list of the first 50 natural frequencies is provided, along with the parameters which are necessary to completely identify the corresponding vibration modes, for both kinematic variables, transversal displacement, V, and cross-sectional rotation, Φ. The plots of some representative modes are also given, to better illustrate the Timoshenko beam response in terms of free vibrations.

Finally, it is useful to point out that this work provides some useful guidelines to study more complex problems. A first interesting example is the case of curved Timoshenko beams which have been tackled by using the isogeometric approach: in particular, for 1D structures some works have been recently published [52–58]. Also the use of mixed and hybrid methods and of highly efficient discretization techniques, such as those reported in [59–61], is promising. All of them provide more accurate stress description and therefore may improve the relevant numerical results. Geometric nonlinear phenomena and dynamic effects can be explored, too, by using, respectively, the tools reported in [62–71]; for wave propagation problems in second gradient continua and micromorphic materials see also [72–76].

Furthermore, the Timoshenko beam model, being a particularly simple micro-mechanical model, is able to furnish fruitful clues about developing new and refined mathematical models of continua, see for instance, the current research trend on generalized continua and their applications [77–89], taking also into account the suggestions presented in [90–92].

Finally, an accurate evaluation of the spectrum is fundamental in problems which consider damage detection, see [93–96], or which drive the response of smart structures, see [97,98].

Acknowledgments

The financial support of MIUR, the Italian Ministry of Education, University and Research, under Grant PRIN 2010–2011 (Project 2010MBJK5B—*Dynamic, Stability and Control of Flexible Structures*) is gratefully acknowledged.

Appendix A. Analysis of the wave-number equation

To investigate the nature of the eigensolutions, it is essential to check whether the roots of the biquadratic Eq. (2.19) are either real or complex conjugates. In particular, the following steps have to be performed.

1. identifying the sign of the discriminant $\hat{\Delta} = \hat{b}^2 - 4\hat{c}$;
2. verifying whether $\lambda_2^{\star 2} > 0$ or $\lambda_2^{\star 2} = 0$ or $\lambda_2^{\star 2} < 0$;
3. verifying whether $\lambda_1^{\star 2} > 0$ or $\lambda_1^{\star 2} = 0$ or $\lambda_1^{\star 2} < 0$.

Preliminarily, it can be stated that all material properties, as well as cross-sectional data, have to be positive for physical reasons. Now the above-mentioned tasks will be accomplished in the afore-listed order.

1. First, attention is concentrated on the sign of the discriminant. Then, taking account of Eqs. (2.20) and (2.21), it is possible to show that:

$$\hat{\Delta} = \frac{\rho^2\omega^4}{E^2}\left(1+\frac{E}{G\kappa}\right)^2 - 4\frac{\rho^2\omega^4}{E^2}\frac{E}{G\kappa} + 4\frac{\rho\omega^2 A}{EI} = \frac{\rho^2\omega^4}{E^2}\left(1-\frac{E}{G\kappa}\right)^2 + 4\frac{\rho\,\omega^2 A}{EI} > 0. \tag{A.1}$$

So the discriminant $\hat{\Delta}$, being the sum of positive quantities, never becomes negative.

Moreover $\hat{\Delta} = 0$ implies either $\omega^2 = 0$ or

$$\omega^2 = -\frac{\frac{4EA}{\rho I}}{\left(1-\frac{E}{G\kappa}\right)^2} < 0. \tag{A.2}$$

Hence $\hat{\Delta}$ vanishes only for *one value* of $\omega \in \mathbb{R}$, namely $\omega = 0$.

It follows from here that the two roots $\lambda_1^{\star 2}$, $\lambda_2^{\star 2}$ defined by Eq. (2.22) do coincide only when $\omega = 0$. For such value, it is simply:

$$\lambda_1^{\star 2} = \lambda_2^{\star 2} = -\frac{\hat{b}}{2}|_{\omega=0} = 0. \tag{A.3}$$

2. As a consequence, since the sum of two negative quantities cannot be positive, it follows that $\lambda_2^{\star 2} \leq 0$, and $\lambda_2^{\star 2} = 0$ *only when* $\omega = 0$; in all other instances, it is strictly $\lambda_2^{\star 2} < 0$.

3. Finally, it is required investigating the sign of $\lambda_1^{\star 2}$. By substitution, it can be written in this equivalent form:

$$\lambda_1^{\star 2} = -\frac{\rho\omega^2}{2E}\left(1+\frac{E}{G\kappa}\right) + \sqrt{\frac{\rho^2\omega^4}{4E^2}\left(1-\frac{E}{G\kappa}\right)^2 + \frac{\rho\omega^2 A}{EI}}. \tag{A.4}$$

It is now an easy task checking that:

$$\lambda_1^{\star 2} > 0 \Rightarrow \sqrt{\frac{\rho^2\omega^4}{4E^2}\left(1-\frac{E}{G\kappa}\right)^2 + \frac{\rho\omega^2 A}{EI}} > \frac{\rho\omega^2}{2E}\left(1+\frac{E}{G\kappa}\right), \tag{A.5}$$

and since both the rhs and the lhs of expression (A.5) are strictly positive, inequality is preserved if they are squared. Thus, after canceling common terms on both sides of the inequality, it follows that:

$$\frac{A}{I} > \frac{\rho\omega^2}{G\kappa} \Rightarrow \omega^2 < \frac{G\kappa A}{\rho I} = \tilde{\omega}^2.$$

Hence, the conclusion for item 3 above is:

$$\begin{aligned} &\lambda_1^{\star 2} > 0 \quad \text{if} \quad \omega^2 < \tilde{\omega}^2, \\ &\lambda_1^{\star 2} = 0 \quad \text{if} \quad \omega^2 = \tilde{\omega}^2, \\ &\lambda_1^{\star 2} < 0 \quad \text{if} \quad \omega^2 > \tilde{\omega}^2. \end{aligned} \tag{A.6}$$

In conclusion, according to the value assumed by ω^2 with reference to $\tilde{\omega}^2$, three different cases have to be distinguished.

Appendix B. Deduction of the frequency equation for the simply supported beam

By Eqs. (2.20), (2.21), $(2.22)_2$ and $(3.12)_2$, this equivalent expression for ω is obtained:

$$\sqrt{\frac{\rho^2\omega^4}{4E^2}\left(1-\frac{E}{G\kappa}\right)^2 + \frac{\rho\omega^2 A}{EI}} = \left(\frac{k_2\pi}{L}\right)^2 - \frac{\rho\omega^2}{2E}\left(1+\frac{E}{G\kappa}\right). \tag{B.1}$$

The right- and left-hand sides of this equation can be squared, giving an equivalent expression, *only if they have the same sign*, i.e. provided that:

$$\left(\frac{k_2\pi}{L}\right)^2 - \frac{\rho\omega^2}{E}\left(1+\frac{E}{G\kappa}\right) > 0,$$

and the result is:

$$\frac{\rho}{2E}\left(1+\frac{E}{G\kappa}\right)\omega^2 < \left(\frac{k_2\pi}{L}\right)^2. \tag{B.2}$$

Since, by Eq. (2.6), the factor multiplying ω^2 in Eq. (B.2) can be given this form:

$$D = \frac{1}{2}\frac{\rho}{E}\left(1+\frac{E}{G\kappa}\right) = \frac{1}{2}\left(\frac{d}{c}+\frac{b}{a}\right), \tag{B.3}$$

where $D > 0$ is a constant, independent of k_2, it follows that Eq. (B.2) is equivalent to imposing this upper bound on the value of ω^2 corresponding to a given value of index k_2:

$$\omega^2 < \frac{1}{D}\left(\frac{k_2\pi}{L}\right)^2 = {\omega_{k_2}^{\star}}^2. \tag{B.4}$$

In particular, Eq. (B.4) requires eliminating $k_2 = 0$ from the set of admissible values, since it would give a negative value for ω^2.

By squaring both sides of Eq. (B.1) and after some rearrangements, the following result is obtained:

$$\omega^4 - \frac{G\kappa}{\rho}\left[\frac{A}{I} + \left(\frac{k_2\pi}{L}\right)^2\left(1 + \frac{E}{G\kappa}\right)\right]\omega^2 + \frac{EG\kappa}{\rho^2}\left(\frac{k_2\pi}{L}\right)^4 = 0. \tag{B.5}$$

A final compact form of Eq. (B.5) is arrived at, if the following shorthand notation is adopted:

$$b^\star = -\frac{G\kappa}{\rho}\left[\frac{A}{I} + \left(\frac{k_2\pi}{L}\right)^2\left(1 + \frac{E}{G\kappa}\right)\right], \quad c^\star = \frac{EG\kappa}{\rho^2}\left(\frac{k_2\pi}{L}\right)^4, \tag{B.6}$$

producing as a result the biquadratic equation:

$$\omega^4 + b^\star\omega^2 + c^\star = 0.$$

Appendix C. Analysis of the frequency equation

The same procedure presented in Appendix A is here used for investigating the solutions, Eq. (3.14), of the frequency equation for the simply supported beam, Eq. (3.13):

1. The sign of the discriminant $\Delta^\star = b^{\star 2} - 4c^\star$;
2. For which values of the parameters $\omega_1^2 > 0$ and satisfies the requirement expressed by Eq. (B.2);
3. For which values of the parameters $\omega_2^2 > 0$ and satisfies the requirement expressed by Eq. (B.2).

The analysis proceeds as follows:

1. It can be easily verified that $\Delta^\star$ might be written equivalently as:

$$\Delta^\star = \left(\frac{G\kappa}{\rho}\right)^2\left[\left(\frac{A}{I}\right)^2 + 2\frac{A}{I}\left(1 + \frac{E}{G\kappa}\right)\left(\frac{k\pi}{L}\right)^2 + \left(1 - \frac{E}{G\kappa}\right)^2\left(\frac{k\pi}{L}\right)^4\right].$$

Now, $\Delta^\star > 0$, since it comes out to be the sum of positive values only.

2. Since $\Delta^\star > 0$ it is also true, by virtue of Eq. $(3.14)_1$, (B.6), that $\omega_1^2 > 0$ *for all possible values of the parameters.*

However, with reference to the requirement expressed by Eq. (B.2) it can be shown, after some lengthy computations, that it is equivalent to imposing:

$$\frac{G\kappa}{4E}\left[\left(1 + \frac{E}{G\kappa}\right)\frac{A}{I} + \left(1 - \frac{E}{G\kappa}\right)^2\left(\frac{k_2\pi}{L}\right)^2\right] + \frac{\rho}{4E}\left(1 + \frac{E}{G\kappa}\right)\sqrt{\Delta^\star} < 0,$$

which is impossible, since the sum of addends which are always positive never produces a negative number. Hence the value $\omega_1^2 > 0$ *is not admissible* in the present case.

3. The condition $\omega_2^2 > 0$ requires that $-b^\star > \Delta^\star$ and can be stated in this equivalent form:

$$\left[\frac{A}{I} + \left(1 + \frac{E}{G\kappa}\right)\left(\frac{k_2\pi}{L}\right)^2\right] > \sqrt{\left[\left(\frac{A}{I}\right)^2 + 2\frac{A}{I}\left(1 + \frac{E}{G\kappa}\right)\left(\frac{k_2\pi}{L}\right)^2 + \left(1 - \frac{E}{G\kappa}\right)^2\left(\frac{k_2\pi}{L}\right)^4\right]}$$

and after some algebraic manipulation it can be reduced to the condition:

$$\left(1 + \frac{E}{G\kappa}\right)^2 > \left(1 - \frac{E}{G\kappa}\right)^2,$$

which is always satisfied.

Moreover, the frequency value given by ω_2^2 is *fully admissible*, since it can be shown to satisfy also the requirement given by Eq. (B.2). Indeed, after some cumbersome algebra it turns out:

$$\left[2\frac{A}{I}\left(\frac{k_2\pi}{L}\right)^2\left(1+\frac{E}{G\kappa}\right)^2+\left(\frac{k_2\pi}{L}\right)^4\left(1-\frac{E}{G\kappa}\right)^2\right]\left[\left(1-\frac{E}{G\kappa}\right)^2-\left(1+\frac{E}{G\kappa}\right)^2\right]<0,$$

which is always satisfied, since the last term within square brackets is always negative.

Appendix D. The frequency equation for the simply supported beam in the second part of the spectrum

It is necessary to recall that, by substituting (2.20), (2.21), $(2.22)_1$ and $(3.29)_1$ this equivalent expression for ω is found:

$$\sqrt{\frac{\rho^2\omega^4}{4E^2}\left(1-\frac{E}{G\kappa}\right)^2+\frac{\rho\,\omega^2 A}{EI}}=\frac{\rho\omega^2}{2E}\left(1+\frac{E}{G\kappa}\right)-\left(\frac{k_1\pi}{L}\right)^2. \tag{D.1}$$

The rhs and lhs of this equation can be squared, as usual, only if they have the same sign:

$$\frac{\rho\omega^2}{E}\left(1+\frac{E}{G\kappa}\right)-\left(\frac{k_1\pi}{L}\right)^2>0,$$

and the result is:

$$\frac{\rho}{2E}\left(1+\frac{E}{G\kappa}\right)\omega^2>\left(\frac{k_1\pi}{L}\right)^2. \tag{D.2}$$

If Eq. (B.3) is recalled, the following lower bound for ω^2 as a function of index k_1 is established:

$$\omega^2>\frac{1}{D}\left(\frac{k_1\pi}{L}\right)^2=\omega_{k_1}^{\star\,2}. \tag{D.3}$$

By squaring both sides of Eq. (D.1) and after performing some rearrangements, the same *frequency equation* for the simply supported Timoshenko beam is obtained:

$$\omega^4-\frac{G\kappa}{\rho}\left[\frac{A}{I}+\left(\frac{k_1\pi}{L}\right)^2\left(1+\frac{E}{G\kappa}\right)\right]\omega^2+\frac{EG\kappa}{\rho^2}\left(\frac{k_1\pi}{L}\right)^4=0, \tag{D.4}$$

see Eq. (B.5), with the simple substitution of k_1 in the position previously hold by k_2. Clearly, in this case, admissible solutions for ω_1^2 must comply with the requirement expressed by Eq. (D.3).

References

1. Timoshenko, S.P.: On the correction for shear of the differential equation for transverse vibrations of prismatic bars. Philos. Mag. (Ser. 5) **41**, 744–746 (1921)
2. Timoshenko, S.P.: On the transverse vibrations of bars of uniform cross-section. Philos. Mag. (Ser. 5) **43**, 125–131 (1922)
3. Stefan, J.: Über die Transversalschwingungen eines elastischen Stabes. K.K. Hof- und Staatsdruckerei, Wien (1858)
4. Rayleigh, J.W.S.B.: The Theory of Sound, vol. 1. Macmillan and Co., London (1877)
5. Han, S.M., Benaroya, H., Wei, T.: Dynamics of transversely vibrating beams using four engineering theories. J. Sound Vib. **225**, 935–988 (1999)
6. Labuschagne, A., Rensburg, N.F.J.van , Merwe, A.J. van der : Comparison of linear beam theories. Math. Comput. Model. **49**, 20–30 (2009)
7. Karnopp, B.H.: Duality relations in the analysis of beam oscillations. Z. Angew. Math. Phys. (ZAMP) **18**, 575–580 (1967)
8. Tabarrok, B., Karnopp, B.H.: Analysis of the oscillations of the Timoshenko beam. Z. Angew. Math. Phys. (ZAMP) **18**, 580–587 (1967)
9. Eisley, J.G.: Nonlinear vibration of beams and rectangular plates. Z. Angew. Math. Phys. (ZAMP) **15**, 167–175 (1964)

10. Traill-Nash, R.W., Collar, A.R.: The effects of shear flexibility and rotatory inertia on the bending vibrations of beams. Q. J. Mech. Appl. Math. **6**, 186–222 (1953)
11. Downs, B.: Transverse vibration of a uniform, simply supported Timoshenko beam without transverse deflection. J. Appl. Mech. **43**, 671–674 (1976)
12. Abbas, B.A.H., Thomas, J.: The second frequency spectrum of Timoshenko beams. J. Sound Vib. **51**, 123–137 (1977)
13. Bhashyam, G.R., Prathap, G.: The second frequency spectrum of Timoshenko beams. J. Sound Vib. **76**, 407–420 (1981)
14. Levinson, M., Cooke, D.W.: On the two frequency spectra of Timoshenko beams. J. Sound Vib. **84**, 319–326 (1982)
15. Stephen, N.G.: The second frequency spectrum of Timoshenko beams. J. Sound Vib. **80**, 578–582 (1982)
16. Prathap, G.: The two frequency spectra of timoshenko beams—a re-assessment. J. Sound Vib. **90**, 443–445 (1983)
17. Levinson, M.: Author's reply. J. Sound Vib. **90**, 445–446 (1983)
18. Nesterenko, V.V.: A theory for transverse vibrations of the Timoshenko beam. J. Appl. Math. Mech. **57**, 669–677 (1993)
19. Nesterenko, V.V., Chervyakov, A.M.: Parabolic approximation to the theory of transverse vibrations of rods and beams. J. Appl. Mech. Tech. Phys. **35**, 306–309 (1994)
20. Olsson, P., Kristensson, G.: Wave splitting of the Timoshenko beam equation in the time domain. Z. Angew. Math. Phys. (ZAMP) **45**, 866–881 (1994)
21. Ekwaro-Osire, S., Maithripala, D.H.S., Berg, J.M.: A series expansion approach to interpreting the spectra of the Timoshenko beam. J. Sound Vib. **240**, 667–678 (2001)
22. Stephen, N.G.: The second spectrum of Timoshenko beam theory—further assessment. J. Sound Vib. **292**, 372–389 (2006)
23. Stephen, N.G., Puchegger, S.: On the valid frequency range of Timoshenko beam theory. J. Sound Vib. **297**, 1082–1087 (2006)
24. Bhaskar, A.: Elastic waves in Timoshenko beams: the 'lost and found' of an eigenmode. Proc. R. Soc. A Math. Phys. Eng. Sci. **465**, 239–255 (2009)
25. Senjanović, I., Vladimir, N.: Physical insight into Timoshenko beam theory and its modification with extension. Struct. Eng. Mech. **48**(4), 519–545 (2013)
26. van Rensburg, N.F.J., van der Merwe, A.J.: Natural frequencies and modes of a Timoshenko beam. Wave Motion **44**, 58–69 (2006)
27. Pilkey, W.D.: Formulas for Stress, Strain, and Structural Matrices, 2nd edn. Wiley, Hoboken (2005)
28. Reddy, J.N.: Mechanics of Laminated Composite Plates and Shells: Theory and Analysis, 2nd edn. CRC Press, Boca Raton (2003)
29. Karnowsky, I.A., Lebed O.I.: Formulas for Structural Dynamics—Tables, Graphs and Solutions. McGraw-Hill, New York (2001)
30. Cazzani, A., Stochino, F., Turco, E.: An analytical assessment of finite element and isogeometric analyses of the whole spectrum of Timoshenko beams. J. Appl. Math. Mech./Z. Angew. Math. Mech. (ZAMM), pp. 1–25 (2016, accepted)
31. Graff, K.F.: Wave Motion in Elastic Solids. Oxford University Press, London (1975)
32. Cazzani, A., Stochino, F., Turco, E.: On the whole spectrum of Timoshenko beams. Part II: further applications. Z. Angew. Math. Phys. (ZAMP), pp. 1–21 (2016). doi:10.1007/s00033-015-0596-9
33. Goens, E.: Über die Bestimmung des Elastizitätsmoduls von Stäben mit Hilfe von Biegungsschwingungen. Ann. Phys. (Ser. 5) **403**, 649–678 (1931)
34. Föppl, A.: Vorlesungen über technische Mechanik—Dritter Band: Festigkeitslehre. B.G. Teubner, Leipzig (1897)
35. Kaneko, T.: On Timoshenko's correction for shear in vibrating beams. J. Phys. D Appl. Phys. **8**, 1927–1936 (1975)
36. Jensen, J.J.: On the shear coefficient in Timoshenko's beam theory. J. Sound Vib. **87**, 621–635 (1983)
37. Renton, J.D.: A note on the form of the shear coefficient. Int. J. Solids Struct. **34**, 1681–1685 (1997)
38. Méndez-Sánchez, R.A., Morales, A., Flores, J.: Experimental check on the accuracy of Timoshenko's beam theory. J. Sound Vib. **279**, 508–512 (2005)
39. Dong, S.B., Alpdogan, C., Taciroglu, E.: Much ado about shear correction factors in Timoshenko beam theory. Int. J. Solids Struct. **47**, 1651–1665 (2010)
40. Cowper, G.R.: The shear coefficient in Timoshenko's beam theory. J. Appl. Mech. **33**, 335–340 (1966)
41. Higuchi, S., Saito, H., Hashimoto, C.: A study of the approximate theory of an elastic thick beam. Can. J. Phys. **35**(6), 757–765 (1957)
42. Hutchinson, J.R.: Shear coefficients for Timoshenko beam theory. J. Appl. Mech. **68**, 87–92 (2001)
43. Stephen, N.G.: On the variation of Timoshenko's shear coefficient with frequency. J. Appl. Mech. **45**, 695–697 (1978)
44. Stephen, N.G.: On "A check on the accuracy of Timoshenko's beam theory". J. Sound Vib. **257**, 809–812 (2002)
45. Chan, K.T., Lai, K.F., Stephen, N.G., Young, K.: A new method to determine the shear coefficient of Timoshenko beam theory. J. Sound Vib. **330**, 3488–3497 (2011)
46. Rosinger, H.E., Ritchie, I.G.: On Timoshenko's correction for shear in vibrating isotropic beams. J. Phys. D Appl. Phys. **10**(08), 1461–1466 (1977)
47. Doyle, P.F., Pavlovic, M.N.: Vibration of beams on partial elastic foundations. Earthq. Eng. Struct. Dyn. **10**, 663–674 (1982)

48. Eisenberger, M., Yankelevsky, D.Z., Adin, M.A.: Vibrations of beams fully or partially supported on elastic foundations. Earthq. Eng. Struct. Dyn. **13**, 651–660 (1985)
49. Cazzani A.: On the dynamics of a beam partially supported by an elastic foundation: An exact solution-set. Int. J. Struct. Stab. Dyn. 13:1350045 (2013). doi:10.1142/S0219455413500454
50. Levinson, M.: Free vibrations of a simply supported, rectangular plate: an exact elasticity solution. J. Sound Vib. **98**, 289–298 (1985)
51. Stephen, N.G.: Mindlin plate theory: best shear coefficient and higher spectra validity. J. Sound Vib. **202**, 539–553 (1997)
52. Cazzani, A., Malagù, M., Turco, E.: Isogeometric analysis of plane-curved beams. Math. Mech. Solids (2014). doi:10.1177/1081286514531265
53. Cazzani, A., Malagù, M., Turco E.: Isogeometric analysis: a powerful numerical tool for the elastic analysis of historical masonry arches. Contin. Mech. Thermodyn. **28**(1–2), 139–156 (2016)
54. Cazzani, A., Malagù, M., Turco, E., Stochino, F.: Constitutive models for strongly curved beams in the frame of isogeometric analysis. Math. Mech. Solids **21**(2), 182–209 (2016)
55. Chiozzi, A., Malagù, M., Tralli, A., Cazzani A.: ArchNURBS: NURBS-based tool for the structural safety assessment of masonry arches in MATLAB. J. Comput. Civ. Eng. (2015). doi:10.1061/(ASCE)CP.1943-5487.0000481
56. Cuomo, M., Contrafatto, L., Greco, L.: A variational model based on isogeometric interpolation for the analysis of cracked bodies. Int. J. Eng. Sci. **80**, 173–188 (2014)
57. Greco, L., Cuomo, M.: An implicit G^1 multi patch B-spline interpolation for Kirchhoff-Love space rod. Comput. Methods Appl. Mech. Eng. **269**, 173–197 (2014)
58. Greco, L., Cuomo, M.: B-spline interpolation of Kirchhoff–Love space rods. Comput. Methods Appl. Mech. Eng. **256**, 251–269 (2013)
59. Cazzani, A., Garusi, E., Tralli, A., Atluri, S.N.: A four-node hybrid assumed-strain finite element for laminated composite plates. Comput. Mater. Contin. **2**, 23–38 (2005)
60. Bilotta, A., Formica, G., Turco, E.: Performance of a high-continuity finite element in three-dimensional elasticity. Int. J. Numer. Methods Biomed. Eng. (Commun. Numer. Methods Eng.) **26**, 1155–1175 (2010)
61. Turco, E., Caracciolo, P.: Elasto-plastic analysis of Kirchhoff plates by high simplicity finite elements. Comput. Methods Appl. Mech. Eng. **190**, 691–706 (2000)
62. Rizzi, N., Varano, V., Gabriele, S.: Initial postbuckling behavior of thin-walled frames under mode interaction. Thin Walled Struct. **68**, 124–134 (2013)
63. Gabriele, S., Rizzi, N., Varano, V.: A 1D higher gradient model derived from Koiter's shell theory. Math. Mech. Solids (2014). doi:10.1177/1081286514536721
64. Rizzi, N., Varano, V.: The effects of warping on the postbuckling behaviour of thin-walled structures. Thin Walled Struct. **49**(9), 1091–1097 (2011)
65. Zulli, D., Luongo, A.: Bifurcation and stability of a two-tower system under wind-induced parametric, external and self-excitation. J. Sound Vib. **331**(2), 365–383 (2012)
66. Pignataro, M., Rizzi, N., Ruta, G., Varano, V.: The effects of warping constraints on the buckling of thin-walled structures. J. Mech. Mater. Struct. **4**(10), 1711–1727 (2009)
67. Ruta, G.C., Varano, V., Pignataro, M., Rizzi, N.L.: A beam model for the flexural–torsional buckling of thin-walled members with some applications. Thin Walled Struct. **46**(7–9), 816–822 (2008)
68. Presta, F., Hendy, C.R., Turco, E.: Numerical validation of simplified theories for design rules of transversely stiffened plate girders. Struct. Eng. **86**(21), 37–46 (2008)
69. Piccardo, G., Ranzi, G., Luongo, A.: A complete dynamic approach to the generalized beam theory cross-section analysis including extension and shear modes. Math. Mech. Solids **19**(8), 900–924 (2014)
70. Piccardo, G., Tubino, F., Luongo, A.: Equivalent nonlinear beam model for the 3-D analysis of shear-type buildings: application to aeroelastic instability. Int. J. Nonlinear Mech. (2015). doi:10.1016/j.ijnonlinmec.2015.07.013
71. Del Vescovo, D., Giorgio, I.: Dynamic problems for metamaterials: review of existing models and ideas for further research. Int. J. Eng. Sci. **80**, 153–172 (2014)
72. dell'Isola, F., Madeo, A., Placidi, L.: Linear plane wave propagation and normal transmission and reflection at discontinuity surfaces in second gradient 3D continua. J. Appl. Math. Mech./Z. Angew. Math. Mech. (ZAMM) **92**(1), 52–71 (2012)
73. Berezovski, A., Giorgio, I., Della Corte, A.: Interfaces in micromorphic materials: wave transmission and reflection with numerical simulations. Math. Mech. Solids (2015). doi:10.1177/1081286515572244
74. Madeo, A., Neff, P., Ghiba, I.-D., Placidi, L., Rosi, G.: Band gaps in the relaxed linear micromorphic continuum. J. Appl. Math. Mech./Z. Angew. Math. Mech. (ZAMM) **95**(9), 880–887 (2015)
75. Madeo, A., Neff, P., Ghiba, I.D., Placidi, L., Rosi, G.: Wave propagation in relaxed micromorphic continua: modeling metamaterials with frequency band-gaps. Contin. Mech. Thermodyn. **27**(4–5), 551–570 (2015)
76. Placidi, L., Rosi, G., Giorgio, I., Madeo, A.: Reflection and transmission of plane waves at surfaces carrying material properties and embedded in second-gradient materials. Math. Mech. Solids (2013). doi:10.1177/1081286512474016

77. dell'Isola, F., Lekszycki, T., Pawlikowski, M., Grygoruk, R., Greco, L.: Designing a light fabric metamaterial being highly macroscopically tough under directional extension: first experimental evidence. Z. Angew. Math. Phys. (ZAMP) (2015). doi:10.1007/s00033-015-0556-4
78. Andreaus, U., Giorgio, I., Madeo, A.: Modeling of the interaction between bone tissue and resorbable biomaterial as linear elastic materials with voids. Z. Angew. Math. Phys. (ZAMP) **66**(1), 209–237 (2015)
79. Grillo, A., Federico, S., Wittum, G.: Growth, mass transfer, and remodeling in fiber-reinforced, multi-constituent materials. Int. J. Nonlinear Mech. **47**(2), 388–401 (2012)
80. Federico, S., Grillo, A., Imatani, S., Giaquinta, G., Herzog, W.: An energetic approach to the analysis of anisotropic hyperelastic materials. Int. J. Eng. Sci. **46**, 164–181 (2008)
81. Alibert, J.-J., Della Corte, A.: Second-gradient continua as homogenized limit of pantographic microstructured plates: a rigorous proof. Z. Angew. Math. Phys. (ZAMP) **66**, 2855–2870 (2015)
82. dell'Isola, F., Andreaus, U., Placidi, L.: At the origins and in the vanguard of peridynamics, non-local and higher-gradient continuum mechanics: an underestimated and still topical contribution of Gabrio Piola. Math. Mech. Solids **20**(8), 887–928 (2015)
83. Yang, Y., Ching, W., Misra, A.: Higher-order continuum theory applied to fracture simulation of nanoscale intergranular glassy film. J. Nanomech. Micromech. **1**(2), 60–71 (2011)
84. dell'Isola, F., Della Corte, A., Giorgio, I., Scerrato, D.: Pantographic 2D sheets: discussion of some numerical investigations and potential applications. Int. J. Nonlinear Mech. (2015). doi:10.1016/j.ijnonlinmec.2015.10.010
85. Rahali, Y., Giorgio, I., Ganghoffer, J.F., dell'Isola, F.: Homogenization à la Piola produces second gradient continuum models for linear pantographic lattices. Int. J. Eng. Sci. **97**, 148–172 (2015)
86. Rahali, Y., Goda, I., Ganghoffer, J.-F.: Numerical identification of classical and nonclassical moduli of 3D woven textiles and analysis of scale effects. Compos. Struct. **135**, 122–139 (2016)
87. Misra, A., Poorsolhjouy, P.: Granular micromechanics model for damage and plasticity of cementitious materials based upon thermomechanics. Math. Mech. Solids (2015). doi:10.1177/1081286515576821
88. Carcaterra, A., dell'Isola, F., Esposito, R., Pulvirenti, M.: Macroscopic description of microscopically strongly inhomogenous systems: A mathematical basis for the synthesis of higher gradients metamaterials. Arch. Ration. Mech. Anal. **218**(3), 1239–1262 (2015)
89. Neff, P., Ghiba, I.-D., Madeo, A., Placidi, L., Rosi, G.: A unifying perspective: the relaxed linear micromorphic continuum. Contin. Mech. Thermodyn. **26**(5), 639–681 (2014)
90. Eremeyev, V.A., Pietraszkiewicz, W.: Local symmetry group in the general theory of elastic shells. J. Elast. **85**, 125–152 (2006)
91. Eremeyev, V.A., Pietraszkiewicz, W.: Material symmetry group of the non-linear polar-elastic continuum. Int. J. Solids Struct. **49**, 1993–2005 (2012)
92. Challamel, N., Kocsis, A., Wang, C.M.: Discrete and non-local elastica. Int. J. Nonlinear Mech. **77**, 128–140 (2015)
93. Roveri, N., Carcaterra, A.: Damage detection in structures under travelling loads by the Hilbert–Huang transform. Mech. Syst. Signal Process. **28**, 128–144 (2012)
94. Bilotta, A., Turco, E.: A numerical study on the solution of the Cauchy problem in elasticity. Int. J. Solids Struct. **46**, 4451–4477 (2009)
95. Bilotta, A., Turco E.: Numerical sensitivity analysis of corrosion detection. Math. Mech. Solids (2014). doi:10.1177/1081286514560093
96. Alessandrini, G., Bilotta, A., Morassi, A., Turco, E.: Computing volume bounds of inclusions by EIT measurements. J. Sci. Comput. **33**(3), 293–312 (2007)
97. Buffa, F., Cazzani, A., Causin, A., Poppi, S., Sanna, G.M., Solci, M., Stochino, F., Turco E.: The Sardinia radio telescope: a comparison between close range photogrammetry and FE models. Math. Mech. Solids (2015). doi:10.1177/1081286515616227
98. Stochino, F., Cazzani, A., Poppi, S., Turco, E.: Sardinia radio Telescope finite element model updating by means of photogrammetric measurements. Math. Mech. Solids (2015). doi:10.1177/1081286515616046

Antonio Cazzani
DICAAR—Department of Civil and Environmental Engineering and Architecture
University of Cagliari
2, via Marengo
09123 Cagliari
Italy
e-mail: antonio.cazzani@unica.it

Flavio Stochino and Emilio Turco
DADU—Department of Architecture
Design and Urban Planning
University of Sassari
Asilo Sella,
35, via Garibaldi
07041 Alghero, SS
Italy
e-mail: fstochino@uniss.it; emilio.turco@uniss.it

(Received: November 13, 2015; revised: December 13, 2015)